Non-imaging optics

using Laplacian magic windows and Zernike polynomials

by

Niels Buijssen

to obtain the degree of Bachelor of Science
at the Delft University of Technology,

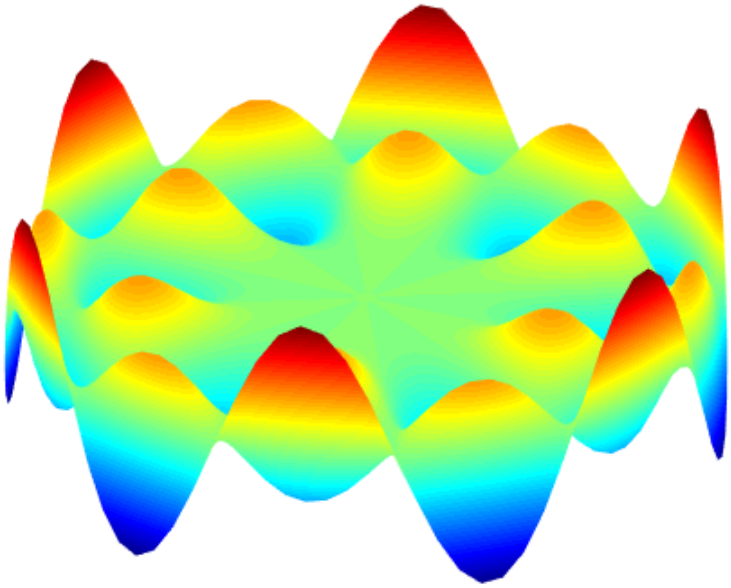

Student number:	4561473	
Project duration:	September, 2018 – July, 2019	
Thesis committee:	Dr. A.J.L. Adam,	TU Delft, supervisor
	Dr. J.L.A. Dubbeldam	TU Delft, supervisor
	Dr. F. Bociort	TU Delft
	Dr. Ir W. Groenevelt	TU Delft

TU Delft

Abstract

In this report a semi-analytic solution to the Laplacian magic window is proposed. The Laplacian magic window is a term recently introduced in 2017[2]. When a uniform wavefront hits a refractive surface, it creates an illumination distribution behind the surface. When the curvature of the surface is sufficiently small, it can be related linearly to the target illumination, and thus creates a 'magic window'. The main idea of the semi-analytic solution is that a target illumination or a surface given in terms of Zernike polynomials can be solved analytically and expressed again in Zernike polynomials. The Zernike polynomials are set of complete and orthogonal polynomials that are already used in the field of optics to describe wavefronts of optical surfaces. The results of the semi-analytic solution agree qualitatively with the numeric results and work for complex and diverse inputs. The implementation is done in 2D, but the method is general enough so it can be extended to 3D.

Preface

This project is the most ambitious academic undertaking for me so far. It is also the accumulation of knowledge and academic skill I accumulated the last three years in my bachelor. Working on this project for a whole year taught me a lot, and I am very grate for the people that supported me. I'd like to thank Aurèle for the supervision and the help he gave me during this project. He was always patient to listen to my problems and suggest solutions. Furthermore I would like to thank Johan for giving me advice on the mathematical part.

Contents

1 Introduction

The field of optics is one with a long history. Already since 1300 there have been glasses to improve eyesight. Nowadays optics still play a vital part in daily life. You are either reading this on a computer screen composed out of LED lights or this document was printed by a laser printer. Classical optics address to problem of creating an image of an object and it's used in many devices such as cameras, mirrors, glasses, and machinery used in the lithography industry. Many advances have been made to improve image quality such as aberration and diffraction corrections, or even adaptive optics. A field that is less explored is that of non-imaging optics. The first thorough introduction was published in 2008 [4]. In this new field, the goal is not to create an image, as the name suggests, but to obtain a certain target illumination. Applications are very wide and useful. Examples are decreasing or increasing the spread of LED lights, improving the design of headlamps in cars and streetlights, creating compact projection display systems, and focusing the concentration of solar energy to increase the yield of solar panels. Non-imaging optics have several advantages over traditional imaging designs: they are more compact, can consist of fewer parts, are better suited to combine light sources from different places and are especially cheap to produce with recent improvements of production techniques such as 3D printing, and can be more robust.

A recent paper in 2017 by Berry [2] introduces a new method to solve non-imaging optics problems. When a uniform wavefront in medium with refractive index greater than one, reaches a transparent surface with air or vacuum behind it, the curvature of the surface can be related to the target intensity behind the surface. More precisely, a linear relation is found between the target intensity and the Laplacian of the surface, if the curvature of the surface is sufficiently small. The direct problem - calculating the intensity given the surface - can be solved straightforwardly numerically with ray tracing techniques. The inverse problem - computing the surface given a target intensity - is a lot harder to solve since calculating the inverse Laplacian is not very straightforward. The paper by Berry does not give a precise technique how to solve this and uses standard numerical methods.

This report aims to solve the direct and indirect problem using a semi-analytic method. The main idea is that an intensity or surface given in terms of Zernike polynomials can be solved analytically and expressed again in Zernike polynomials. The Zernike polynomials are set of complete and orthogonal polynomials that are already used in the field of optics to describe wavefronts of optical surfaces.

In chapter 2, the problem stated above and the solution of Berry will be explained more in depth. In chapter 3, a rigorous mathematical description of the Zernike polynomials will be given, and the application of the Zernike polynomials will be discussed in chapter 4. In chapter 5, the analytic solution will be proposed, along with details of the implementation and comparison to ray tracer solutions and checks. The discussion of the solution and check with numerical results can be found in chapter 6. Chapter 7 contains the conclusion of this report.

This report is part of the thesis project of the double degree program Applied Mathematics and Applied Physics at the TU Delft.

2

Problem and methods

2.1. Introduction

The problem is to find the best optical surface that for a known incident light gives a desired illumination output. This is visualised in figure 2.1.

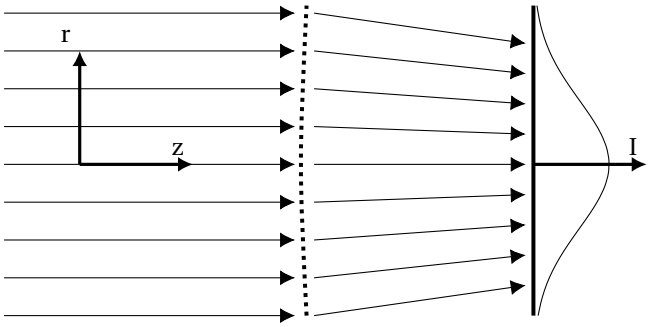

Figure 2.1: General representation of the problem. The dotted lines describe some optical system, and behind the optical system we have an intensity distribution.

As can be seen from figure 2.1 we have collimated beam of light coming from the left. This is passed through an optical system denoted by the dotted line. The light is then propagated to some receiver plane where there will be some intensity distribution. The optical system can in principle consist of an arbitrary number of lenses, mirrors and other optical apparati, but the focus of this report is on a single element with one or two transparent surfaces. The single or double nature is inherent to the methods used as will be discussed. Multiple surfaces have certain advantages, namely that they can correct for aberration and dispersion, and have more precision. This however is beyond the scope of this project.

The direct problem is to find the intensity, given the optical system. The inverse problem would be to find the optical surface, given the intensity. This problem can easily be generalised to go from one intensity problem to another by first solving an inverse problem, giving a collimated beam, and then use the inverse problem to find the second optical system. The final result would be placing the two optical systems behind each other along the optical axis.

It should be noted that all methods used are limited to geometrical optics. It is expected that this will not be a problem because the aperture of the optical system can be chosen large enough that diffraction won't play a big role. Also the accuracy of the system doesn't need to be so accurate as such as the output intensity is only to be observed with naked eye, for example.

2.2. Known techniques

First a few methods will be described that could be used to solve this problem. The methods can sometimes be used only to solve the direct or inverse problem respectively, or both. Most methods have advantages and

disadvantages and these will be discussed. This section will introduce the methods briefly, but by no means give an extensive way to solve the problem.

2.2.1. Ray tracing

A very straightforward and useful technique is ray tracing. This can of course only be applied to the direct problem. Once the optical system has been found, one can initialise a set of rays, and trace them through the system. In the appendix the following formula is derived for this purpose.

$$\boldsymbol{v_r} = \frac{n_1}{n_2}\boldsymbol{v_i} + \left(\frac{n_1}{n_2}(\boldsymbol{v_i} \bullet \boldsymbol{n})\boldsymbol{n} - \sqrt{1 - \left(\frac{n_1}{n_2}\right)^2 (1 - (\boldsymbol{v_i} \bullet \boldsymbol{n})^2)}\right)\boldsymbol{n}$$

where $\boldsymbol{v_r}$ is the refracted ray and $\boldsymbol{v_i}$ the incoming ray. $\boldsymbol{n}$ is the normal vector of the refractive surface and n_i represent different refractive indices. After the optical system one can easily find, for each ray, its position in space via $r = az + b$ where the parameters a and b can be found with the boundary conditions of the direction of the refracted ray and the position when it leaves the optical system. Then one can make a histogram of the ray density at the output plane in order to obtain the intensity distribution. This is a very useful method since it is very simple and straightforward. Because it can only be applied for the direct case and is computationally heavy, its main purpose is to check and compare solutions found by other methods.

2.2.2. SMS method

The first attempt at solving the inverse problem was the SMS method, which is an acronym for Simultaneous Multiple Surfaces[3]. As the name implies it outputs two, or more, surfaces simultaneously. However, it is restricted to uniform intensities by its nature. As input it takes two planes in three dimensions and finds two surfaces between the planes. These 2 surfaces can be connected in order to produce a lens. The method works by finding points of the lens via an iterative method, and is computationally light. It can be useful for certain applications, when one only cares about uniform intensity. The specific workings of the method can be found in the appendix, along with a worked out example produced by the method.

The SMS method deserves a mention in this report because it solved the problem, but is very limited in use since it has to stick to uniform densities. Therefore others method should be preferred. The next subsection will describe such a method.

2.2.3. Laplacian magic window

The Laplacian magic window is technique coined by Sir Micheal Berry [2] only recently in 2017. If the optical system consists of one surface, it relates its curvature to the intensity behind the lens (linearly) by the Laplacian of the surface. This method works before the first caustic of a system. This is due to the fact that a caustic, where rays cross, give an infinite density of rays. This is not compatible with the method as will now be explained. The following situation is sketched.

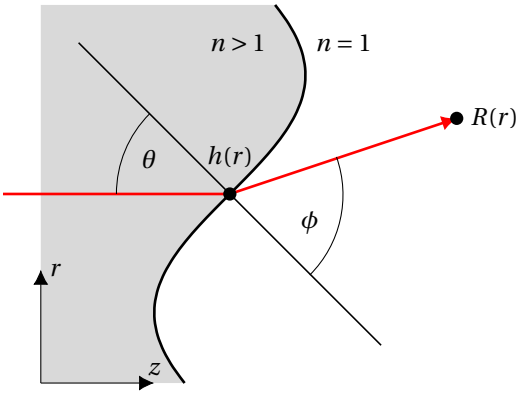

Figure 2.2: Geometry for refraction by a magic window. The curvature is exaggerated for clarity. Based on [2].

Define angles θ and ϕ, coordinates r and z, surface h, and the receiver plane R as in figure 2.2. Then

Snell's law can be used to obtain [2]

$$R(r) = r + (z - h(r))\frac{\tan(\theta - \phi)}{|t(r)|}t(r) \tag{2.1}$$

where $t(r) = \nabla h(r)$ is the transverse gradient of the surface. Then trigonometry leads to[2]

$$\frac{\tan(\theta - \phi)}{|t(r)|} = \frac{n\sqrt{1 - (n^2 - 1)|t(r)|^2} - 1}{1 - (n^2 - 1)|t(r)|^2} \tag{2.2}$$

It is then possible to find the intensity at the image plane via

$$I(R) = \left(\det\left(\frac{\partial R(r)}{\partial r}\right)_{r=r(R)}\right)^{-1} \tag{2.3}$$

where $r(R) = R(r)^{-1}$. Here we can immediately see that $I(R)$ needs to be single valued i.e. no caustics. This means that $h(r)$ needs to be sufficiently small. This can be checked by validating the solution with a ray tracer. Because assume that $h(r)$ is small, we Taylor expand to find

$$R(r) \approx r + z(n-1)\nabla h(r) \tag{2.4}$$

We then neglect the quadratic (∂_{xx} for example) and higher order terms to find

$$I(r) \approx \frac{1}{1 + (n-1)z \triangle h(r)} \tag{2.5}$$

which can again be expanded into a linear relation

$$I(r) \approx 1 - (n-1)z \triangle h(r) \tag{2.6}$$

The paper[2] then goes on by calculating $h(r)$ numerically by standard inverse Laplacian solvers. However, we can use techniques in order to calculate $h(r)$ from equation 2.6 directly. These techniques involve choosing a smart mathematical basis such as using Zernike decomposition. In order to use it more background is needed on the Zernike polynomials, which are used for the Zernike decomposition. That will be described in the next section.

The following figure gives an overview of the problem and solutions we have mentioned so far.

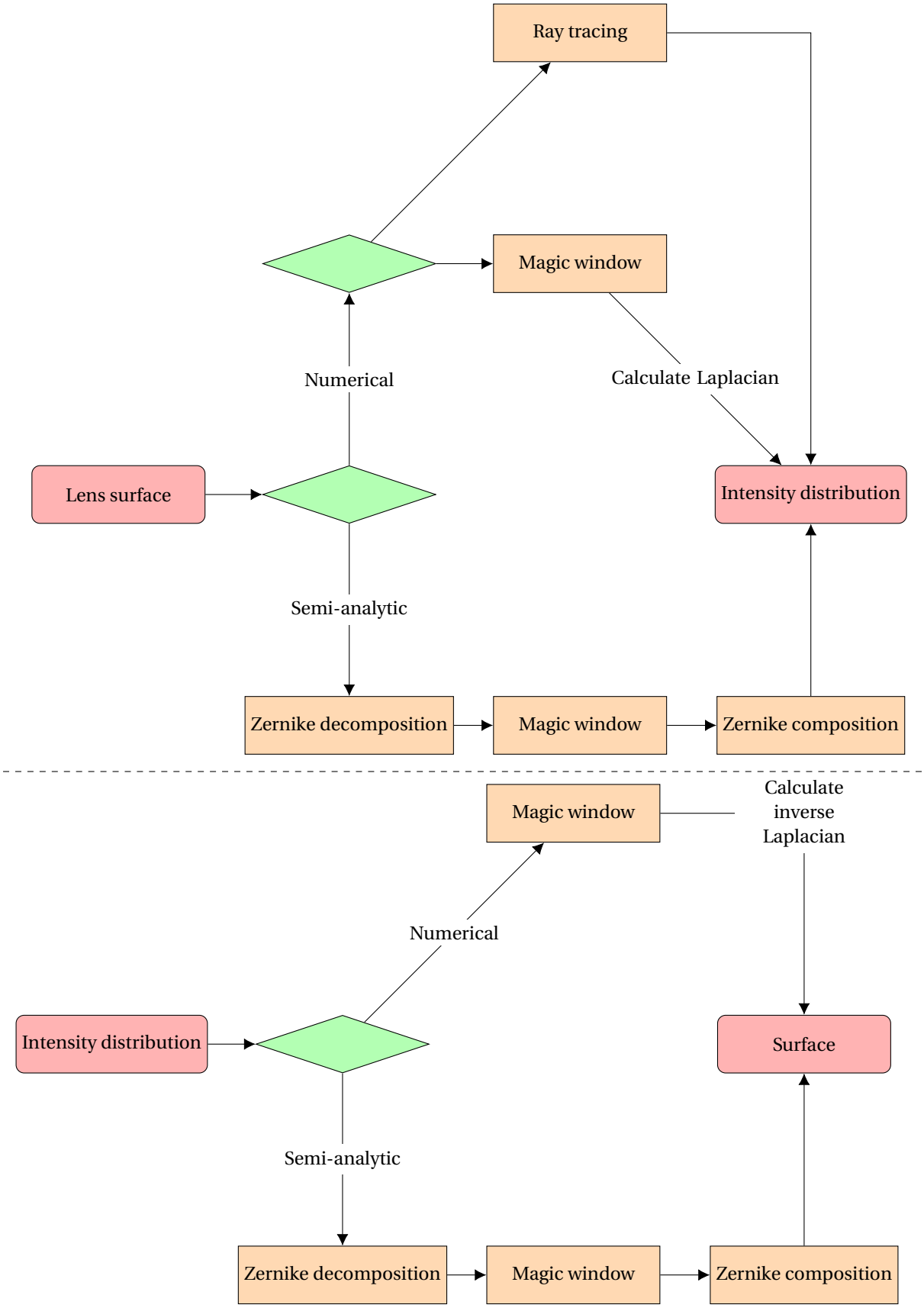

Figure 2.3: Decision chart to solve the direct (upper chart) and inverse (lower chart) problem. Red smoothed rectangles represent starting and stopping nodes. Green diamonds represent a decision and orange rectangles processes.

2.3. Zernike polynomials

The Zernike polynomials are a type of orthogonal polynomials that form a complete set on the unit disc. This makes them a very attractive candidate to describe wave fronts, since a lot of applications in optics are disc or ellipse like. Their orthogonal nature makes them ideal form easily finding the correct coefficients for two reasons. First of all the one can find an explicit expression for the coefficients as will be seen in later chapters. Secondly, if n coefficients are given, and higher order terms are required for greater precision or other reasons, finding the higher order coefficients will not change the value of the first n coefficients because the associated eigenfunctions are linearly independent. However, there are more sets of eigenfunctions that have the same properties. For example the Rogers-Szego polynomials [6]. However, the Zernike polynomials are useful specifically for optics and this report. For optics in general they are very useful to describe wave fronts because the terms of the Zernike polynomials are in the same form as types of aberration often observed in optical tests [12]. Specifically for this report they are useful because they have 'nice' properties. The properties will be more thoroughly discussed in the next chapter, but for now it suffices to know that separation of variables can be done in polar coordinates, they preserve their form if rotated over an arbitrary angle, and they can be expressed in a single infinite sum, rather than 2 sums which can be the case for polynomials in 2 dimensions. Furthermore their relevance for optics led to a lot of research of the Zernike polynomials, which means that a lot of information can be found about them in literature. This makes them an attractive candidate for using them in this report.

It should be noted that Zernike polynomials are not perfect. They cannot describe air turbulence well [12] and they are not orthogonal when only a finite number of points on the unit disc are known. That means that blind use of Zernike polynomials can lead to unforeseen consequences: from not being able to describe the properties you want to test, to numerical errors that can lead to very disastrous representations of reality. In this report care is taken to take these problems into account and make sure they can be neglected as much as possible. A section in chapter 4 will be dedicated to take make sure the coefficients converge so numerical errors are minimised.

The next chapter will go into great depths on how the Zernike polynomials are constructed in order to get a better understanding of them, whilst also doing a lot of the groundwork that is needed in order to introduce a semi-analytic solution to the Laplacian magic window problem.

3

Orthogonal polynomials

In this chapter we will work towards building up the Zernike polynomials. As we will find out, they are complete and orthogonal and defined directly by the Jacobi polynomials $P_k^{(\alpha,\beta)}$. This is why first a look needs to be taken at the Jacobi polynomials in order to understand the Zernike polynomials.

3.1. Definitions of orthogonal polynomials

For completeness we state the definition of orthogonality and orthonormality here [6] since we will refer to these definitions a lot, and build our proofs from the grounds of these concepts.

Definition 3.1.1. ***Orthogonality***. *A set of functions* $\{f_1(x), f_2(x), ..., f_l(x)\}$, *with l finite or infinite, is orthogonal with respect to a weight function* $w(x)$ *if*

$$\int_a^b w(x) f_n(x) f_m(x)\, \mathrm{d}x = h_n \delta_{nm}, \quad \forall n, m \leq l$$

where f_n *belongs to the class* $L^2(a,b)$ *and* h_n *is a constant.*

Definition 3.1.2. ***Orthonormality***. *A set of functions* $f_1(x), f_2(x), ..., f_l(x)$, *with l finite or infinite, is orthonormal with respect to a weight function* $w(x)$ *if it is orthogonal and* $h_{nm} = 1 \quad \forall n, m \leq l$.

The following remark will be very useful in a number of proofs, and is general enough to be included in this section.

Remark. *Let* $\{p_0(x), p_1,(x), ..., p_n(x), ...\}$ *be a set of polynomials where* $p_n(x)$ *is a polynomial of precise degree n and the system* $\{p_n(x)\}$ *is orthonormal. Then every* π_n, *where* π_n *denotes a polynomial of degree n, can be represented as a linear combination of* $\{p_0(x), p_1,(x), ..., p_n(x), ...\}$. *Then every* $p_n(x)$ *is orthogonal to any* π_{n-1}.

3.2. Jacobi polynomials

The Jacobi polynomials share a lot with the Laguerre and Hermite polynomials and are therefore called the classical orthogonal polynomials. A lot of special cases of the classical polynomials are used throughout quantum mechanics, like Legendre and Bessel function, to optics, like the Zernike polynomials, and in many other realms of science. Studying them is in that context a very important field of work. They all share very similar definitions, recurrence relations, and proofs of orthogonality and completeness are very similar for these polynomials. Studying the Jacobi polynomials is very useful because it is so easy to generalise them to other functions. The Jacobi polynomials are defined as follows [6]

Definition 3.2.1. *Let* $a = -1, b = 1, w(x) = (1-x)^\alpha (1+x)^\beta, \alpha > -1, \beta > -1$. *Then, up to a constant factor, the orthogonal polynomial* $p_n(x)$ *is the Jacobi polynomial* $P_n^{(\alpha,\beta)}(x)$.

Most sets of orthogonal polynomials, like the Bessel or Legendre, can be derived from the fact that they are the solutions to a differential equation. This is no different for the Jacobi polynomials.

Theorem 3.2.1. *The Jacobi polynomials satisfy the following linear homogeneous second order differential equation:*

$$(1-x^2)y'' + [\beta - \alpha - (\alpha+\beta+2)x]y' + n(n+\alpha+\beta+1)y = 0 \tag{3.1}$$

Proof. Consider the expression

$$\frac{\mathrm{d}}{\mathrm{d}x}\{(1-x)^{\alpha+1}(1+x)^{\beta+1}y'\}$$

Since y is a π_n the above expression above has the form $(1-x)^\alpha(1+x)^\beta z$ with z a π_n. We claim that $z = cy$ with c a constant. To that end let $\rho(x)$ be an arbitrary π_{n-1}. If we can prove that

$$\int_{-1}^{1} \frac{\mathrm{d}}{\mathrm{d}x}\{(1-x)^{\alpha+1}(1+x)^{\beta+1}y'\}\rho(x)\,\mathrm{d}x = 0$$

we have proved the claim. Integration by parts of the left-hand side of the above equation gives

$$\Big[(1-x)^{\alpha+1}(1+x)^{\beta+1}y\rho(x)\Big]_{-1}^{1} - \int_{-1}^{1}(1-x)^{\alpha+1}(1+x)^{\beta+1}y'\rho'(x)\,\mathrm{d}x = 0 - \int_{-1}^{1}(1-x)^{\alpha+1}(1+x)^{\beta+1}y'\rho'(x)\,\mathrm{d}x$$

where the equality holds since $\alpha+1, \beta+1 \neq 0$. Once again using integration by parts gives

$$-\Big[(1-x)^{\alpha+1}(1+x)^{\beta+1}y\rho'(x)\Big]_{-1}^{1} + \int_{-1}^{1} y\frac{\mathrm{d}}{\mathrm{d}x}\{(1-x)^{\alpha+1}(1+x)^{\beta+1}\rho'(x)\}\,\mathrm{d}x = 0 + \int_{-1}^{1} y\frac{\mathrm{d}}{\mathrm{d}x}\{(1-x)^{\alpha+1}(1+x)^{\beta+1}\rho'(x)\}\,\mathrm{d}x$$

The coefficient of y in this last integrand is $\frac{\mathrm{d}}{\mathrm{d}x}\{(1-x)^{\alpha+1}(1+x)^{\beta+1}\rho'(x)\}$ which is of the form $(1-x)^\alpha(1+x)^\beta r(x)$ with r a π_{n-1}. Hence the integral vanishes and the claim follows. In theorem 3.2.2 it is found that $c = -n(n+\alpha+\beta+1)$. The following equation combines everything we have found

$$\frac{\mathrm{d}}{\mathrm{d}x}\{(1-x)^{\alpha+1}(1+x)^{\beta+1}y'\} = -n(n+\alpha+\beta+1)(1-x)^\alpha(1+x)^\beta y \tag{*}$$

Using the chain rule on the left-hand side of the above equation gives

$$\begin{aligned}
\text{l.h.s.}(*) &= \frac{\mathrm{d}}{\mathrm{d}x}\{(1-x)^{\alpha+1}\}(1+x)^{\beta+1}y' + \frac{\mathrm{d}}{\mathrm{d}x}\{(1+x)^{\beta+1}\}(1-x)^{\alpha+1}y' + \frac{\mathrm{d}}{\mathrm{d}x}\{y'\}(1-x)^{\alpha+1}(1+x)^{\beta+1} \\
&= (1-x)^\alpha(1+x)^\beta(\alpha+1)(1+x)y' + (1-x)^\alpha(1+x)^\beta(\beta+1)(1-x)y' + (1-x)^\alpha(1+x)^\beta(1-x)(1+x)y'' \\
&= (1-x)^\alpha(1+x)^\beta\left[y'((\alpha+1)(1+x) + (\beta+1)) + y''(1-x)(1+x)\right] \\
&= (1-x)^\alpha(1+x)^\beta\left[y'(\beta-\alpha-(\alpha+\beta+2)x) + y''(1-x^2)\right] \qquad (**)
\end{aligned}$$

Because $\alpha, \beta > -1$, the expression $(1-x)^\alpha(1+x)^\beta$ never becomes zero or infinite[1] so we can combine equation (*) and (**) and divide by $(1-x)^\alpha(1+x)^\beta$ to prove the theorem. □

Theorem 3.2.2. *Let $\alpha > -1, \beta > -1$. Then the differential equation*

$$(1-x^2)y'' + [\beta - \alpha - (\alpha+\beta+2)x]y' + \gamma y = 0$$

where γ is a parameter, has a non trivial polynomial solution if and only if $\gamma = n(n+\alpha+\beta+1)$ with $n \in \mathbb{N}_{>0}$. This solution is $cP_n^{(\alpha,\beta)}(x)$, with c a constant, and no solution which is linearly independent of $P_n^{(\alpha,\beta)}(x)$ can be a polynomial.

[1] The relevant interval is $(-1,1)$ and not $[-1,1]$

Proof. Let $y = \sum_{\nu=0}^{\infty} a_\nu (x-1)^\nu$. Then $y' = \sum_{\nu=0}^{\infty} \nu a_\nu (x-1)^{\nu-1}$ and $y'' = \sum_{\nu=0}^{\infty} \nu(\nu-1) a_\nu (x-1)^{\nu-2}$

$$(1-x^2)\sum_{\nu=0}^{\infty} \nu(\nu-1)a_\nu(x-1)^{\nu-2} + [\beta-\alpha-(\alpha+\beta+2)x]\sum_{\nu=0}^{\infty} \nu a_\nu (x-1)^{\nu-1} + \gamma\sum_{\nu=0}^{\infty} a_\nu(x-1)^\nu = 0 \tag{3.2}$$

$$-(1+x)\sum_{\nu=0}^{\infty} \nu(\nu-1)a_\nu(x-1)^{\nu-1} - [2(\alpha+1)+(\alpha+\beta+2)(x-1)]\sum_{\nu=0}^{\infty} \nu a_\nu (x-1)^{\nu-1} + \gamma\sum_{\nu=0}^{\infty} a_\nu(x-1)^\nu = 0 \tag{3.3}$$

$$-((x-1)+2)\sum_{\nu=0}^{\infty} \nu(\nu-1)a_\nu(x-1)^{\nu-1} - \sum_{\nu=0}^{\infty} [2\nu(\alpha+1)-\gamma+\nu(\alpha+\beta+2)(x-1)]a_\nu(x-1)^{\nu-1} = 0 \tag{3.4}$$

$$-\sum_{\nu=1}^{\infty} 2[\nu(\nu-1)+\nu(\alpha+1)]a_\nu(x-1)^{\nu-1} + \sum_{\nu=0}^{\infty}[\gamma-\nu(\nu+\alpha+\beta+1)]a_\nu(x-1)^\nu = 0 \tag{3.5}$$

$$-\sum_{\nu=0}^{\infty} 2(\nu+1)(\nu+\alpha+1)a_{\nu+1}(x-1)^\nu + \sum_{\nu=0}^{\infty}[\gamma-\nu(\nu+\alpha+\beta+1)]a_\nu(x-1)^\nu = 0 \tag{3.6}$$

which yields the recurrence formula

$$[\gamma-\nu(\nu+\alpha+\beta+1)]a_\nu = 2(\nu+1)(\nu+\alpha+1)a_{\nu+1} \tag{3.7}$$

Now assume that y is a polynomial and a_n the last non zero coefficient. That means that the left-hand side of equation 3.7 must vanish and we find $\gamma = n(n+\alpha+\beta+1)$. Since coefficient of a_{n+1} never vanishes, we find that $a_m = 0 \quad \forall m > n$.
For the second part of the proof, we let z be a second solution to equation 3.1. Consider the expression

$$(1-x)^{\alpha+1}(1+x)^{\beta+1}(y'z - yz') \tag{3.8}$$

From theorem 3.2.1 we know that this equals a constant for all $x \in [-1,1]$. Taking $x \to \pm 1$ we can see that this constant equals zero. That means the Wronskian $W(y,z) = 0$ almost everywhere on the relevant interval. We see that y and z cannot both be polynomials unless the constant in the right member is zero, that is, unless y and z are linearly dependent. □

3.2.1. Hypergeometric functions

We have found a way to tie a unique differential equation to the Jacobi polynomials. In the next section we will rewrite this differential equation into a form that we know the solution of. Specifically the solutions will be the hypergeometric functions.

In equation 3.1 substitute $x = 1-2z$. Then $\mathrm{d}x = -2\,\mathrm{d}z$ and we find

$$(1-x^2)y'' + [\beta-\alpha-(\alpha+\beta+2)x]y' + n(n+\alpha+\beta+1)y = 0 \tag{3.9}$$

$$(1-(1-2z)^2)\frac{\mathrm{d}^2 y}{\mathrm{d}(1-2z)^2} + [\beta-\alpha-(\alpha+\beta+2)(1-2z)]\frac{\mathrm{d}y}{\mathrm{d}(1-2z)} + n(n+\alpha+\beta+1)y = 0 \tag{3.10}$$

$$(4z-4z^2)\frac{\mathrm{d}^2 y}{4\,\mathrm{d}z^2} + [-2\alpha-2+2(\alpha+\beta+2)z]\frac{\mathrm{d}y}{-2\,\mathrm{d}z} + n(n+\alpha+\beta+1)y = 0 \tag{3.11}$$

$$z(1-z)\frac{\mathrm{d}^2 y}{\mathrm{d}z^2} + [\alpha+1-(\alpha+\beta+2)z]\frac{\mathrm{d}y}{\mathrm{d}z} + n(n+\alpha+\beta+1)y = 0 \tag{3.12}$$

which can be recognised as the hypergeometric equation of Gauss

$$z(1-z)\frac{\mathrm{d}^2 w}{\mathrm{d}z^2} + [c-(a+b-1)z]\frac{\mathrm{d}w}{\mathrm{d}z} - abw = 0. \tag{3.13}$$

The solution is the hypergeometric function[2] defined for $|z| < 1$ by the power series

$$F(a;b;c;z) = \sum_{\nu=0}^{\infty} \frac{(a)_\nu (b)_\nu}{(c)_\nu}\frac{z^\nu}{\nu!}. \tag{3.14}$$

[2] I could have chosen to derive this as well, but my project is finite. I think to keep the focus on the Jacobi polynomials, this is a good moment to refer to literature.

It is undefined if c equals a non-positive integer. Here $(q)_\nu$ is the rising Pochhammer symbol defined as

$$(q)_\nu = \begin{cases} 1 & \nu = 0 \\ q(q+1)...(q+\nu-1) & \nu > 0 \end{cases} \tag{3.15}$$

Using the second part of theorem 3.2.2 we find the important representation

$$P_n^{(\alpha,\beta)}(z) = \binom{n+\alpha}{n} F(-n; n+\alpha+\beta+1; \alpha+1; \frac{1-z}{2}) \tag{3.16}$$

Where the constant c has been replaced with $\binom{n+\alpha}{n}$. This constant can be determined by the normalisation factor

$$P_n^{(\alpha,\beta)}(1) = \binom{n+\alpha}{n} \tag{3.17}$$

The series terminates if either a or b is a non-positive integer, in which case the function reduces to a polynomial

$$F(-m, b; c; z) = \sum_{\nu=0}^{m} (-1)^\nu \binom{m}{\nu} \frac{(b)_\nu}{(c)_\nu} z^\nu \tag{3.18}$$

We can combine everything we know to obtain an explicit expression for the Jacobi polynomials.

$$P_n^{(\alpha,\beta)}(x) = \frac{1}{n!} \sum_{\nu=0}^{n} \binom{n}{\nu} (n+\alpha+\beta+1)\dots(n+\alpha+\beta+\nu)(\alpha+\nu+1)\dots(\alpha+n) \left(\frac{x-1}{2}\right)^\nu. \tag{3.19}$$

A useful corollary for generating functions is 3.2.2.1. To find an expression for the derivative in the same basis is obviously useful and from this corollary many other relations with the derivative can be found.

Corollary 3.2.2.1. *Let $P_n^{(\alpha,\beta)}(x)$ the Jacobi polynomials. Then the following equation holds*

$$\frac{\mathrm{d}}{\mathrm{d}x}\{P_n^{(\alpha,\beta)}(x)\} = \frac{1}{2}(n+\alpha+\beta+1) P_{n-1}^{(\alpha+1,\beta+1)}(x) \tag{3.20}$$

Proof. Apply equation 3.19 to the left-hand side of the formula above

$$\begin{aligned}
\frac{\mathrm{d}}{\mathrm{d}x}\{P_n^{(\alpha,\beta)}(x)\} &= \frac{\mathrm{d}}{\mathrm{d}x}\{\frac{1}{n!} \sum_{\nu=0}^{n} \binom{n}{\nu} (n+\alpha+\beta+1)\dots(n+\alpha+\beta+\nu)(\alpha+\nu+1)\dots(\alpha+n) \left(\frac{x-1}{2}\right)^\nu\} \\
&= \frac{1}{n!} \sum_{\nu=0}^{n} \binom{n}{\nu} \frac{1}{2}\nu(n+\alpha+\beta+1)\dots(n+\alpha+\beta+\nu)(\alpha+\nu+1)\dots(\alpha+n) \left(\frac{x-1}{2}\right)^{\nu-1} \\
&= \frac{1}{2}(n+\alpha+\beta+1)\frac{1}{(n-1)!} \sum_{\nu=0}^{n-1} \binom{n-1}{\nu} \frac{1}{2}\nu(n+\alpha+\beta)\dots(n+\alpha+\beta+\nu)(\alpha+\nu+1)\dots(\alpha+n-1) \left(\frac{x-1}{2}\right)^\nu \\
&= \frac{1}{2}(n+\alpha+\beta+1) P_{n-1}^{(\alpha+1,\beta+1)}(x)
\end{aligned}$$

□

3.2.2. Generalised product rule

We state the generalised product rule and give a proof because it will be required in the proof of theorem 3.2.4. The generalised product rule is also referred to as the Leibniz' rule.

Theorem 3.2.3. ***Generalised product rule.*** *Let f and g be n times differentiable. Then the product fg is also n times differentiable and the n-th derivative is given by*

$$(fg)^{(n)}(x) = \sum_{k=0}^{n} \binom{n}{k} f^{(n-k)}(x) g^{(k)}(x). \tag{3.21}$$

Proof. We will proof theorem 3.2.3 by induction. The induction basis is $n = 1$. Then equation 3.21 reduces to

$$(fg)^{(1)} = f'g + g'f \tag{3.22}$$

which is the well known product rule. For the induction step we assume equation 3.21 to hold for an arbitrary n, then

$$\begin{aligned}
(fg)^{(n+1)} &= \left[\sum_{k=0}^{n}\binom{n}{k}f^{(n-k)}g^{(k)}\right]' && (3.23)\\
&= \sum_{k=0}^{n}\binom{n}{k}f^{(n+1-k)}g^{(k)} + \sum_{k=0}^{n}\binom{n}{k}f^{(n-k)}g^{(k+1)} && (3.24)\\
&= \sum_{k=0}^{n}\binom{n}{k}f^{(n+1-k)}g^{(k)} + \sum_{k=1}^{n+1}\binom{n}{k-1}f^{(n+1-k)}g^{(k)} && (3.25)\\
&= \binom{n}{0}f^{(n+1)}g + \sum_{k=1}^{n}\binom{n}{k}f^{(n+1-k)}g^{(k)} + \sum_{k=1}^{n}\binom{n}{k-1}f^{(n+1-k)}g^{(k)} + \binom{n}{n}fg^{(n+1)} && (3.26)\\
&= f^{(n+1)}g + \left(\sum_{k=1}^{n}\left[\binom{n}{k-1} + \binom{n}{k}\right]f^{(n+1-k)}g^{(k)}\right) + fg^{(n+1)} && (3.27)\\
&= f^{(n+1)}g + \sum_{k=1}^{n}\binom{n+1}{k}f^{(n+1-k)}g^{(k)} + fg^{(n+1)} && (3.28)\\
&= \sum_{k=0}^{n+1}\binom{n+1}{k}f^{(n+1-k)}g^{(k)}. && (3.29)
\end{aligned}$$

So the statement also holds for $n+1$. This completes the induction step and thus the proof. □

3.2.3. Rodrigues' formula

A different, but equivalent, definition is given by Olinde Rodrigues (1865). It is a very useful formula and can be used to obtain various relations.

Theorem 3.2.4. ***Rodrigues' formula.*** *Let $\alpha > -1$, $\beta > -1$. Then*

$$(1-x)^{\alpha}(1+x)^{\beta}P_n^{(\alpha,\beta)}(x) = \frac{(-1)^n}{2^n n!}\left(\frac{\mathrm{d}}{\mathrm{d}x}\right)^n\{(1-x)^{n+\alpha}(1+x)^{n+\beta}\}. \tag{3.30}$$

Proof. The proof will be very similar to the proof of theorem 3.2.1. Consider the expression

$$\left(\frac{\mathrm{d}}{\mathrm{d}x}\right)^n\{(1-x)^{n+\alpha}(1+x)^{n+\beta}\}. \tag{3.31}$$

Using the generalised product rule we find this expression equals

$$\begin{aligned}
&\sum_{k=0}^{n}\binom{n}{k}[(1-x)^{n+\alpha}]^{(n-k)}[(1+x)^{n+\beta}]^{(k)}\\
&\quad= [(1-x)^{n+\alpha}]^{(n)}[(1+x)^{n+\beta}]^{(0)} + \sum_{k=1}^{n-1}\binom{n}{k}[(1-x)^{n+\alpha}]^{(n-k)}[(1+x)^{n+\beta}]^{(k)} + [(1-x)^{n+\alpha}]^{(0)}[(1+x)^{n+\beta}]^{(n)}\\
&\quad= (-1)^n[n+\alpha]_n(1-x)^{\alpha}(1+x)^{\beta}(1+x)^n + \sum_{k=1}^{n-1}\cdots + [n+\beta]_n(1-x)^{\alpha}(1+x)^{\beta}(1-x)^n\\
&\quad= (1-x)^{\alpha}(1+x)^{\beta}\rho_1(x) + \sum_{k=1}^{n-1}\cdots + (1-x)^{\alpha}(1+x)^{\beta}\rho_n(x)\\
&\quad= (1-x)^{\alpha}(1+x)^{\beta}\rho_1(x) + (1-x)^{\alpha}(1+x)^{\beta}\rho_2(x) + \sum_{k=2}^{n-2}\cdots + (1-x)^{\alpha}(1+x)^{\beta}\rho_{n-1}(x) + (1-x)^{\alpha}(1+x)^{\beta}\rho_n(x)\\
&\quad\vdots\\
&\quad= (1-x)^{\alpha}(1+x)^{\beta}\rho(x)
\end{aligned}$$

Here $\rho_i(x)$ is a π_n and $[q]_\nu$ denotes the falling Pochhammer symbol:

$$[q]_\nu = \begin{cases} 1 & \nu = 0 \\ q(q-1)...(q-\nu+1) & \nu > 0 \end{cases} \tag{3.32}$$

Similar to the proof of theorem 3.2.1, to show that $\rho(x) = cP_n^{(\alpha,\beta)}(x)$, it suffices to proof that

$$\int_{-1}^{1} \left(\frac{\mathrm{d}}{\mathrm{d}x}\right)^n \{(1-x)^{\alpha+n}(1+x)^{\beta+n}\} r(x)\,\mathrm{d}x = 0 \tag{3.33}$$

where $r(x)$ is an arbitrary π_{n-1}. To that end we use integration by parts n times

$$\begin{aligned}
&\int_{-1}^{1} \left(\frac{\mathrm{d}}{\mathrm{d}x}\right)^n \{(1-x)^{\alpha+n}(1+x)^{\beta+n}\} r(x)\,\mathrm{d}x \\
&\qquad = \left[\left(\frac{\mathrm{d}}{\mathrm{d}x}\right)^{n-1} \{(1-x)^{\alpha+n}(1+x)^{\beta+n}\} r(x)\right]_{-1}^{1} - \int_{-1}^{1} \left(\frac{\mathrm{d}}{\mathrm{d}x}\right)^{n-1} \{(1-x)^{\alpha+n}(1+x)^{\beta+n}\} r^{(1)}(x)\,\mathrm{d}x \\
&\qquad = 0 - \int_{-1}^{1} \left(\frac{\mathrm{d}}{\mathrm{d}x}\right)^{n-1} \{(1-x)^{\alpha+n}(1+x)^{\beta+n}\} r^{(1)}(x)\,\mathrm{d}x \\
&\qquad = \left[\left(\frac{\mathrm{d}}{\mathrm{d}x}\right)^{n-2} \{(1-x)^{\alpha+n}(1+x)^{\beta+n}\} r(x)^{(1)}\right]_{-1}^{1} + \int_{-1}^{1} \left(\frac{\mathrm{d}}{\mathrm{d}x}\right)^{n-2} \{(1-x)^{\alpha+n}(1+x)^{\beta+n}\} r^{(2)}(x)\,\mathrm{d}x \\
&\qquad = 0 + \int_{-1}^{1} \left(\frac{\mathrm{d}}{\mathrm{d}x}\right)^{n-2} \{(1-x)^{\alpha+n}(1+x)^{\beta+n}\} r^{(2)}(x)\,\mathrm{d}x \\
&\qquad \vdots \\
&\qquad = (-1)^n \int_{-1}^{1} (1-x)^{\alpha+n}(1+x)^{\beta+n} r^{(n)}(x)\,\mathrm{d}x
\end{aligned}$$

which vanishes since $r(x)$ is a π_{n-1} so $r^{(n)}(x) = 0$. Now let $x \to 1$, then we can find the constant

$$\begin{aligned}
c &= \lim_{x\to 1} \frac{1}{P_n^{(\alpha,\beta)}(x)} \frac{1}{(1-x)^\alpha (1+x)^\beta} \left(\frac{\mathrm{d}}{\mathrm{d}x}\right)^n \{(1-x)^{\alpha+n}(1+x)^{\beta+n}\} \\
&= \lim_{x\to 1} \frac{1}{P_n^{(\alpha,\beta)}(x)} \frac{1}{(1-x)^\alpha (1+x)^\beta} \left((-1)^n [n+\alpha]_n (1-x)^\alpha (1+x)^\beta (1+x)^n + \sum_{k=1}^{n} \binom{n}{k} [(1-x)^{n+\alpha}]^{(n-k)} [(1+x)^{n+\beta}]^{(k)}\right) \\
&= \frac{1}{P_n^{(\alpha,\beta)}(1)} (-1)^n [n+\alpha]_n 2^n \\
&= \frac{1}{\binom{n+\alpha}{n}} \binom{n+\alpha}{n} (-1)^n n! 2^n \\
&= (-1)^n n! 2^n
\end{aligned}$$

□

It readily follows that using Leibniz' rule on the right-hand side of Rodrigues' formula, we can find other

expressions for the Jacobi polynomials

$$P_n^{(\alpha,\beta)}(x) = 2^{-n}\sum_{\nu=0}^{n}\binom{n+\alpha}{\nu}\binom{n+\beta}{n-\nu}(x-1)^{n-\nu}(x+1)^{\nu} \tag{3.34}$$

$$= \sum_{\nu=0}^{n}\binom{n+\alpha}{n-\nu}\binom{n+\beta}{n}\left(\frac{x-1}{2}\right)^{n-\nu}\left(\frac{x+1}{2}\right)^{n} \tag{3.35}$$

$$= \binom{n+\alpha}{n}\left(\frac{x+1}{2}\right)^{n} F(-n;-n-\beta;\alpha+1;\frac{x-1}{x+1}) \tag{3.36}$$

Furthermore, from Rodrigues' formula, we can immediately see the symmetry relation

$$P_n^{(\alpha,\beta)}(-x) = (-1)^n P_n^{(\beta,\alpha)}(x) \tag{3.37}$$

Next we will try to find the coefficients so that we can find a orthonormal set associated with the weight function $(1-x)^{\alpha}(1+x)^{\beta}$ on -1.1).

Theorem 3.2.5. *Let $w(x) = (1-x)^{\alpha}(1+x)^{\beta}$ on (-1.1). Then the orthonormal set associated with the weight function $w(x)$ is $p_n(x)$ with*

$$p_n(x) = \left[\frac{2n+\alpha+\beta+1}{2^{\alpha+\beta+1}}\frac{\Gamma(n+1)\Gamma(n+\alpha+\beta+1)}{\Gamma(n+\alpha+1)\Gamma(n+\beta+1)}\right]^{\frac{1}{2}} P_n^{(\alpha,\beta)}(x) \tag{3.38}$$

Proof. We use Rodrigues formula, integration by parts, and the beta function $B(x,y) = \int_0^1 t^{x-1}(1-t)^{y-1}\,\mathrm{d}\,t = \frac{\Gamma(x)\Gamma(y)}{\Gamma(x+y)}$ respectively.

$$\int_{-1}^{1}(1-x)^{\alpha}(1+x)^{\beta}[P_n^{(\alpha,\beta)}(x)]^2\,\mathrm{d}\,x \tag{3.39}$$

$$= l_n^{(\alpha,\beta)}\int_{-1}^{1}(1-x)^{\alpha}(1+x)^{\beta}P_n^{(\alpha,\beta)}(x)x^n\,\mathrm{d}\,x \tag{3.40}$$

$$= \frac{(-1)^n}{2^n n!}\int_{-1}^{1}\left(\frac{\mathrm{d}}{\mathrm{d}\,x}\right)^n\{(1-x)^{n+\alpha}(1+x)^{n+\beta}\}P_n^{(\alpha,\beta)}(x)\,\mathrm{d}\,x \tag{3.41}$$

$$= \frac{(-1)^{2n}}{2^n n!}\int_{-1}^{1}(1-x)^{n+\alpha}(1+x)^{n+\beta}\left(\frac{\mathrm{d}}{\mathrm{d}\,x}\right)^n\{P_n^{(\alpha,\beta)}(x)\}\,\mathrm{d}\,x \tag{3.42}$$

$$= \frac{(-1)^{2n}}{2^n n!}\int_{-1}^{1}(1-x)^{n+\alpha}(1+x)^{n+\beta}d_{n,n}^{(\alpha,\beta)}P_0^{(\alpha+n,\beta+n)}(x)\,\mathrm{d}\,x \tag{3.43}$$

$$= \frac{2n+\alpha+\beta+1}{2^{\alpha+\beta+1}}\frac{\Gamma(n+1)\Gamma(n+\alpha+\beta+1)}{\Gamma(n+\alpha+1)\Gamma(n+\beta+1)} \tag{3.44}$$

where $d_{n,k}^{(\alpha,\beta)} = \frac{\Gamma(n+k+\alpha+\beta+1)}{2^k\Gamma(n+\alpha+\beta+1)}$ and is obtained by using corollary 3.2.2.1 k times. □

So we have found an orthonormal set of eigenfunctions on the interval $(0,1)$ for the differential equation 3.1. We acquire completeness from the fact that differential equation 3.1 is in fact a Sturm-Liouville problem. I will not discuss this further since this is out of the scope of this project. Interested readers can find more about this[7]. Now we are ready to use this set to describe functions on a unit disc. This is where the Zernike polynomials come into play.

3.3. Zernike polynomials

The Zernike polynomials play an important part in optics, since they are orthogonal over the unit disc. This section will look at the mathematical part - definitions, recurrence relations, theorems - of the Zernike polynomials, whilst the next chapter will look into the application of the polynomials.
The Zernike polynomials $Z_n^m(r,\theta)$ are defined as

$$Z_n^m(r,\theta) = \begin{cases} R_n^m(r)\cos m\theta & m \geq 0 \\ R_n^m(r)\sin m\theta & m < 0 \end{cases} \tag{3.45}$$

where the radial function $R_n^m(r)$ is given by

$$R_n^m(r) = (-1)^{(n-m)/2} r^m P_{(n-m)/2}^{(m,0)}(1-2r^2) \tag{3.46}$$

and it can be seen that they are directly linked to the Jacobi polynomials. Furthermore the only 'interesting' part is the radial function, since the azimuthal part is 'just' an exponential. That is why most theorems will focus on the radial function.

In the special case that the input of the Jacobi polynomials is real and that $k, k+\alpha, k+\beta$ and $k+\alpha+\beta$ are non-negative integers equation 3.35 reduces to

$$P_k^{(\alpha,\beta)}(x) = (k+\alpha)!(k+\beta)! \sum_s \frac{1}{s!(k+\alpha-s)!(\beta+s)!(k-s)!} \left(\frac{x-1}{2}\right)^{k-s} \left(\frac{x+1}{2}\right)^s \tag{3.47}$$

The radial function is a polynomial of degree $2n$ and can be written as

$$R_n^m(r) = \sum_{s=0}^{(n-|m|)/2} (-1)^s \frac{(n-s)!}{s!\,((n+|m|)/2-s)!\,((n-|m|)/2-s)!} r^{n-2s} \tag{3.48}$$

where $r \in [0,1]$, $n \geq m$ and $n-m$ even.
One can write the Zernike polynomials also in Cartesian coordinates, but this will not be useful for our application, so I refrain from doing so. Interested readers can find more about this in literature[11][9].

3.3.1. Orthogonality

We have claimed many times the Zernike polynomials are orthogonal. Now we have enough background to finally prove this. The proof will also result in an expression of the orthogonality constant, which is very important to find the Zernike coefficients which will become clear next chapter.

Theorem 3.3.1. *Let R_n^m denote the radial function of the Zernike polynomials. Then the functions are orthogonal and have normalisation constant $\sqrt{\frac{1}{2(n+1)}}$.*

$$\int_0^1 R_n^m(r) R_{n'}^m(r) r \,\mathrm{d}\, r = \frac{1}{2(n+1)} \delta_{nn'} \tag{3.49}$$

Proof. My approach is to use theorem and try to work towards an expression for the radial part. We start from the orthogonality condition

$$\int_{-1}^1 w(x) p_k(x) p_k(x) \,\mathrm{d}\, x = \delta_{kk'} \tag{3.50}$$

$$\int_{-1}^1 (1-x)^\alpha (1+x)^\beta P_k^{(\alpha,\beta)}(x) P_{k'}^{(\alpha,\beta)}(x) \,\mathrm{d}\, x = h_k^2 \delta_{kk'} \tag{3.51}$$

where $h_k^2 = \left(\frac{2k+\alpha+\beta+1}{2^{\alpha+\beta+1}} \frac{\Gamma(k+1)\Gamma(k+\alpha+\beta+1)}{\Gamma(k+\alpha+1)\Gamma(k+\beta+1)}\right)^{-1}$. We substitute the parameters in the Jacobi polynomials that corresponds with the Zernike polynomials: $\alpha = m$, $\beta = 0$, $k = (n-m)/2$. Orthogonality should be clear and I care

mostly about the orthogonality constant so I will assume, that $k = k'$

$$\int_{-1}^{1} (1-x)^m P^{(m,0)}_{(n-m)/2}(x)^2 \,\mathrm{d}\,x = h_k^2 \tag{3.52}$$

We substitute $x = 1-2r^2$. $\frac{\mathrm{d}\,x}{\mathrm{d}\,r} = \frac{\mathrm{d}}{\mathrm{d}\,r}(1-2r^2) = -4r$. So $\mathrm{d}\,x = -4r\,\mathrm{d}\,r$ and $r(x) = \sqrt{\frac{1-x}{2}}$. The boundaries are then mapped via $r(x)$ as follows: $-1 \mapsto 1, 1 \mapsto 0$. This gives

$$\int_{1}^{0} (1-(1-2r^2))^m P^{(m,0)}_{(n-m)/2}(1-2r^2)^2 \cdot -4r \,\mathrm{d}\,r = h_k^2 \tag{3.53}$$

$$2^{m+2} \int_{0}^{1} r^{2m+1} P^{(m,0)}_{(n-m)/2}(1-2r^2)^2 \,\mathrm{d}\,r = h^2_{(n-m)/2} = \frac{2}{n+1} 2^m \tag{3.54}$$

$$\int_{0}^{1} r^{2m+1} P^{(m,0)}_{(n-m)/2}(1-2r^2)^2 \,\mathrm{d}\,r = \frac{1}{2(n+1)} \tag{3.55}$$

$$\int_{0}^{1} r^{2m+1} P^{(m,0)}_{(n-m)/2}(1-2r^2)^2 \,\mathrm{d}\,r = \tag{3.56}$$

$$\int_{0}^{1} (-1)^{2k} r^{2m} P^{(m,0)}_{(n-m)/2}(1-2r^2)^2 r \,\mathrm{d}\,r = \tag{3.57}$$

$$\int_{0}^{1} \left((-1)^{(n-m)/2} r^m P^{(m,0)}_{(n-m)/2}(1-2r^2)\right)^2 r \,\mathrm{d}\,r = \tag{3.58}$$

$$\int_{0}^{1} R^m_n(r)^2 r \,\mathrm{d}\,r = N^m_n \tag{3.59}$$

So indeed we find the desired result that $N^m_n = \frac{1}{2(n+1)}$. □

The orthogonality conditions of the azimuthal part are rather simple integrals. And I present them without proof

Theorem 3.3.2. *The azimuthal Θ^m_n part of the Zernike polynomials are orthogonal and have normalisation constant $\pi(1+\delta_{m0})\delta_{mm'}$.*

Proof.

$$\int_{0}^{2\pi} \begin{cases} \cos m\theta \cos m'\theta \\ \sin m\theta \sin m'\theta \\ \cos m\theta \sin m'\theta \\ \sin m\theta \cos m'\theta \end{cases} \mathrm{d}\,\theta = \begin{cases} \pi(1+\delta_{m0})\delta_{mm'} \\ \pi\delta_{mm} \\ 0 \\ 0 \end{cases} \tag{3.60}$$

□

Therefore we can combine them to obtain orthogonality

Theorem 3.3.3. *The Zernike polynomials Z^m_n are orthogonal and have normalisation constant $\frac{\pi(1+\delta_{m0})}{2(n+1)}$*

Proof. Using the definition of the Zernike polynomials and applying theorem 3.3.1 and 3.3.2 directly gives the desired result. □

3.3.2. Important relations

To extend the understanding of the Zernike polynomials I will present more proofs of important relations

Theorem 3.3.4. *For the radial function of the Zernike polynomials the following relation holds.*

$$\frac{\mathrm{d}}{\mathrm{d}r}R_n^m(r) = \frac{n^2+m^2-2nr^2}{2nr(1-r^2)}R_n^m(r) - \frac{n^2-m^2}{2nr(1-r^2)}R_{n-2}^m(r) \tag{3.61}$$

Proof. By definition of the Zernike polynomial, and some calculus we find

$$\begin{aligned}(-1)^{(n-m)/2}\frac{\mathrm{d}}{\mathrm{d}r}R_n^m(r) &= \frac{\mathrm{d}}{\mathrm{d}r}\left(r^m P_{(n-m)/2}^{(m,0)}(1-2r^2)\right)\\ &= \frac{\mathrm{d}}{\mathrm{d}r}\left(r^m\right)P_{(n-m)/2}^{(m,0)}(1-2r^2) + r^m\frac{\mathrm{d}(1-2r^2)}{\mathrm{d}r}\frac{\mathrm{d}}{\mathrm{d}(1-2r^2)}\left(P_{(n-m)/2}^{(m,0)}(1-2r^2)\right)\\ &= \frac{m}{r}(-1)^{(n-m)/2}R_n^m(r) - 4r^{m+1}\frac{\mathrm{d}}{\mathrm{d}(1-2r^2)}\left(P_{(n-m)/2}^{(m,0)}(1-2r^2)\right)\end{aligned}$$

This is why we need to find an expression for the derivative of the Jacobi polynomial. This can be found in standard math handbooks [1] equation 22.8.1.

$$(2k+\alpha+\beta)(1-x^2)\frac{\mathrm{d}}{\mathrm{d}x}P_k^{(\alpha,\beta)}(x) = k(\alpha-\beta-x(2k+\alpha+\beta))P_k^{(\alpha,\beta)}(x) + 2(k+\alpha)(k+\beta)P_{k-1}^{(\alpha,\beta)}(x)$$

We fill our new knowledge and find

$$\begin{aligned}\frac{\mathrm{d}}{\mathrm{d}r}R_n^m(r) &= R_n^m(r)\frac{m}{r} - (-1)^{(n-m)/2}4r^{m+1}\cdot\\ &\quad\left(\frac{\frac{n-m}{2}(m-(1-2r^2)(2\frac{n-m}{2}+m))}{n(1-(1-2r^2)^2)}P_{(n-m)/2}^{(m,0)}(1-2r^2) + \frac{2(\frac{n-m}{2}+m)(\frac{n-m}{2})}{n(1-(1-2r^2)^2)}P_{(n-m)/2-1}^{(m,0)}(1-2r^2)\right)\\ &= R_n^m(r)\frac{m}{r} - (-1)^{(n-m)/2}4r^{m+1}\cdot\\ &\quad\left(\frac{\frac{n-m}{2}(m-(1-2r^2)n)}{4nr^2(1-r^2)}P_{(n-m)/2}^{(m,0)}(1-2r^2) + \frac{\frac{1}{2}(n+m)(n-m)}{4nr^2(1-r^2))}P_{(n-2-m)/2}^{(m,0)}(1-2r^2)\right)\\ &= R_n^m(r)\frac{m}{r} - (-1)^{(n-m)/2}r^m\cdot\\ &\quad\left(\frac{(n-m)(m-n(1-2r^2)}{2nr(1-r^2)}P_{(n-m)/2}^{(m,0)}(1-2r^2) + \frac{n^2-m^2}{2nr(1-r^2))}P_{(n-2-m)/2}^{(m,0)}(1-2r^2)\right)\\ &= R_n^m(r)\left(\frac{m}{r} - \frac{(n-m)(m-n(1-2r^2)}{2nr(1-r^2)}\right) - R_{n-2}^m(r)\frac{n^2-m^2}{2nr(1-r^2))}\\ &= R_n^m(r)\left(\frac{n^2+m^2-2n^2r^2}{2nr(1-r^2)}\right) - R_{n-2}^m(r)\frac{n^2-m^2}{2nr(1-r^2))}\end{aligned}$$

□

Theorem 3.3.5. *For the radial function of the Zernike polynomials the following relation holds.*

$$\frac{\mathrm{d}}{\mathrm{d}r}R_n^m(r) = \frac{r^2(n+2)+m}{r(1-r^2)}R_n^m(r) - \frac{n+m+2}{1-r^2}R_{n+1}^{m+1}(r) \tag{3.62}$$

Proof. Proof is similar to theorem 3.3.4 [10] [3]. □

Theorem 3.3.6. *For the radial function of the Zernike polynomials the following relation holds.*

$$R_n^m(r) = \frac{1}{2(n+1)r}\left((n+m+2)R_{n+1}^{m+1} + (n-m)R_{n-1}^{m-1}\right) \tag{3.63}$$

Proof. Proof is similar to theorem 3.3.4 [10]. □

[3] And left as an exercise for the reader

3.3.3. Laplacian

We have discussed in chapter 2 that we will a mathematical trick to quickly solve the Laplacian magic window problem. This trick consists of 2 parts, first of all we need to find the Laplacian of the Zernike polynomials in the same basis, and secondly we need orthogonality. The latter we have already found fortunately. This first attempt to find the Laplacian is to differentiate the summation representation from equation 3.48 twice and add the appropriate terms as via the proof of theorem 3.3.7. Since this is a polynomials we can easily find

$$\triangle R_n^m(r) = \sum_{s=0}^{(n-|m|)/2} (-1)^s \frac{(n-s)!}{s!((n+|m|)/2-s)!((n-|m|)/2-s)!}(n-2s)(n-2s-1)r^{n-2s-2} \tag{3.64}$$

$$+\frac{1}{r}\sum_{s=0}^{(n-|m|)/2} (-1)^s \frac{(n-s)!}{s!((n+|m|)/2-s)!((n-|m|)/2-s)!}(n-2s)r^{n-2s-1} \tag{3.65}$$

$$= \sum_{s=0}^{(n-|m|)/2} (-1)^s \frac{(n-s)!}{s!((n+|m|)/2-s)!((n-|m|)/2-s)!}(n-2s)^2 r^{n-2s-2} \tag{3.66}$$

However, this is not in the same basis as we input in the Laplacian operator so we cannot use it for our purpose. It can however be used to check whether other methods agree with this results to prevent mathematical mistakes or programming errors. A results closer to our desired basis can be found in the following theorem.

Theorem 3.3.7. *The Laplacian of the radial function of the Zernike polynomials is given by*

$$\begin{aligned}\triangle R_n^m(r) = &\frac{1}{r^2(1-r^2)^2}\Big[\\ &R_n^m(r)(r^4(n+2)^2 + 2r^2(m(n+3)+n+2)+m^2) \\ &R_{n+1}^{m+1}(r)r(n+m+2)(r^2(2n+6)+2m+2) \\ &R_{n+2}^{m+2}(r)r^2(n+m+2)(n+m+4) \Big] \\ :=&A(r)R_n^m(r) + B(r)R_{n+1}^{m+1}(r) + D(r)R_{n+2}^{m+2}(r)\end{aligned}$$

Proof. First we invoke the definition of the Laplacian in polar coordinates

$$\triangle f(r) = \left(\frac{\mathrm{d}^2}{\mathrm{d}r^2} + \frac{1}{r}\frac{\mathrm{d}}{\mathrm{d}r}\right) f(r) \tag{3.67}$$

Then theorem 3.62, a little [4] calculus and algebra yields the desired result. □

It should be noted that this still is not in the desired basis as we still have terms with a r dependency in front of the R_n^m terms. This is undesirable and the results section of this report will explain why that is. Another way to find the the Laplacian of the Zernike polynomials was done by Janssen [8]. He found the following expression

$$\triangle Z_n^m(r,\theta) = \sum_{s=|m|(2)(n-2)} (s+1)(n+s+2)(n-s)Z_s^m(r,\theta)$$

Where we introduce the notation

$$i(j)k = i, i+j, i+2j, ..., k-j, k \tag{3.68}$$

Also, the inverse relation was also found

$$\triangle^{-1} Z_n^m(r,\theta) = \frac{1}{4(n+1)(n+2)}Z_{n+2}^m(r,\theta) - \frac{1}{2n(n+2)}Z_n^m(r,\theta) + \frac{1}{4n(n+1)}Z_{n-2}^m(r,\theta)$$

where it should be noted that $\triangle Z_n^m(r,\theta) = 0$ when $n \leq |m|$. The implementation will be discussed further in the results chapter.

[4] Actually it's not a little but extremely much, and extremely tedious.

4

Application of Zernike polynomials

Last chapter constructed a mathematical basis with which we can start to solve the problem. Before before that will be discussed, we focus on understanding the Zernike polynomials through more intuitive means. This chapter aims to connect the abstract ideas to the physical problem described in chapter 2. First of all, the relevance for optics will be discussed, followed by visualising the Zernike polynomials. The last part will discuss computing the Zernike coefficients and numerical reliability.

4.1. Relevance for optics

In general a function $f(r,\theta)$ describing a wavefront in polar coordinates (r,θ) can be expanded as a sequence of orthonormal polynomials P[9]:

$$f(r,\theta) = \sum_{n,m} C_n^m P_n^m(r,\theta)$$

where C is a real coefficient. Zernike polynomials are special because they have three properties other orthogonal sets do not have [11].
First of all, they have simple rotational symmetry:

$$Z(r,\theta) = R(r)\Theta(\theta)$$

where $\Theta(\theta)$ is continuous with period 2π and satisfies the requirement that rotating the coordinate system by α does not change the form of the polynomial:

$$\Theta(\theta+\alpha) = \Theta(\alpha)\Theta(\theta)$$

It is easy to check that the function $\Theta(\theta) = e^{(\pm i m\theta)}$ meets these requirements. The second property is that the radial component $R(r)$ must be of degree $2n$ and contain no power of r less than m.
Thirdly, if m is odd, $R(r)$ must be odd, and if m is even, $R(r)$ must be even.

Combining these properties Z can be written as

$$Z_n^m(r,\theta) = \begin{cases} R_n^m(r)\cos m\theta & m \geq 0 \\ R_n^m(r)\sin m\theta & m < 0 \end{cases} \tag{4.1}$$

Let us take a look at the radial part, since we can use the Jacobi polynomials here. Define the radial part as

$$R_n^m(r) = (-1)^{(n-m)/2} r^m P_{(n-m)/2}^{(m,0)}(1-2r^2)$$

The desired properties of the Zernike polynomials are present as one can easily check.

4.2. Visualising the Zernike polynomials

The next section aims to give an intuition for what the Zernike polynomials represent. We plot a few even and odd parts of the radial function from table 4.1.

n	m	$R_n^m(r)$
1	1	r
2	0	$2r^2-1$
3	1	$3r^3-2r$
4	0	$6r^4-6r^2+1$

Table 4.1: Some of the radial functions of the Zernike polynomials. This set is not complete because for every n there can be $n+1$ values of m: $m=-n,-n+2,...,n-2,n$.

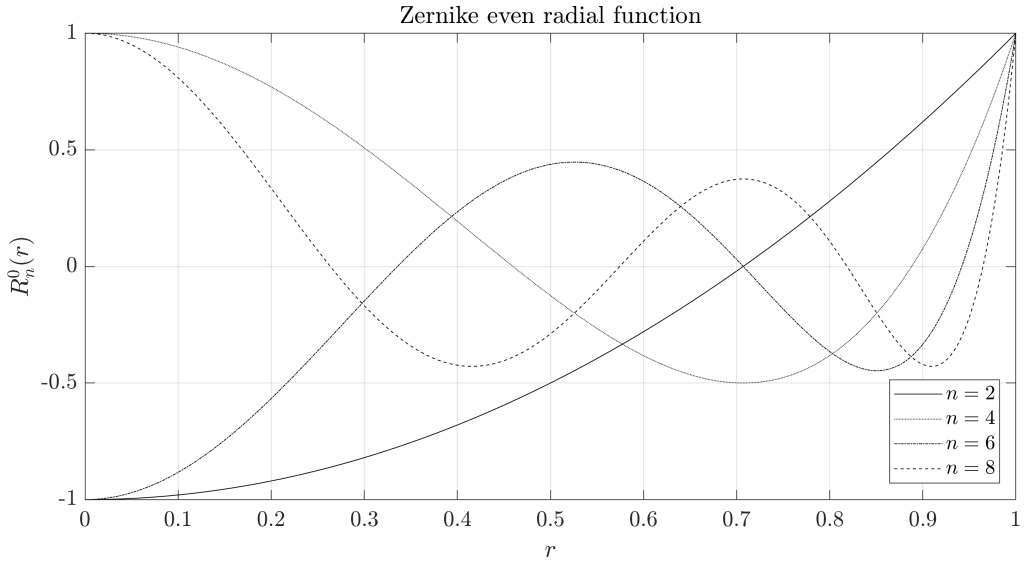

Figure 4.1: Some even parts of the radial Zernike functions. $m=0$ is fixed and n is varied from 2 up to 8. We can clearly see the normalisation $R_n^m(1)=1$.

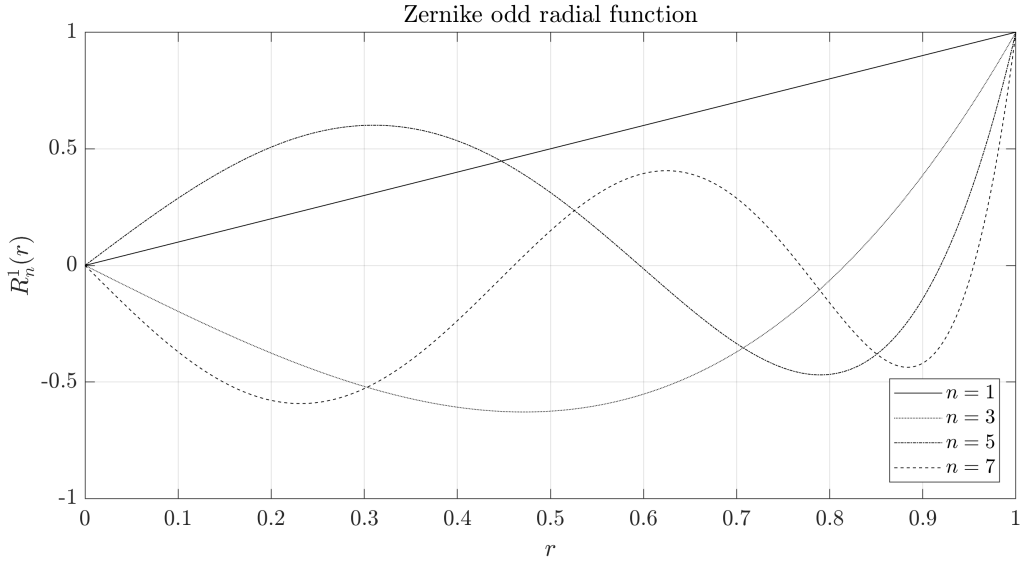

Figure 4.2: Some odd parts of the radial Zernike functions. $m=1$ is fixed and n is varied from 1 up to 7. We can clearly see the normalisation $R_n^m(1)=1$.

For completeness we also show the case n is fixed.

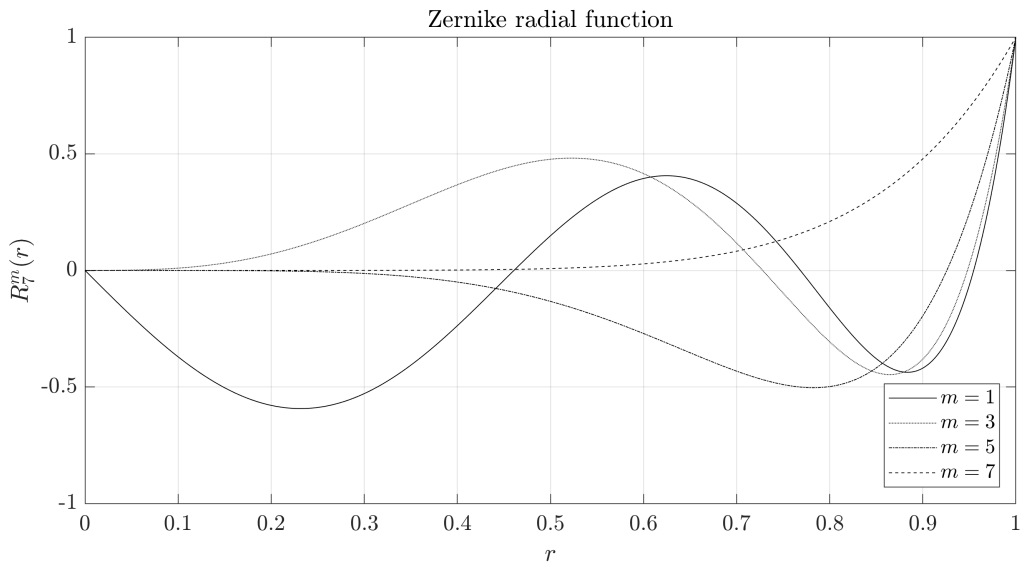

Figure 4.3: Some parts of the radial Zernike functions. $n = 7$ is fixed and m is varied from 1 up to 7. Note that m can also take up negative values, but the radial function is identical: that is $R_n^m(r) = R_n^{-m}(r)$. We can clearly see the normalisation $R_n^m(1) = 1$.

We can also visualise the Zernike polynomials in 3 dimensions.

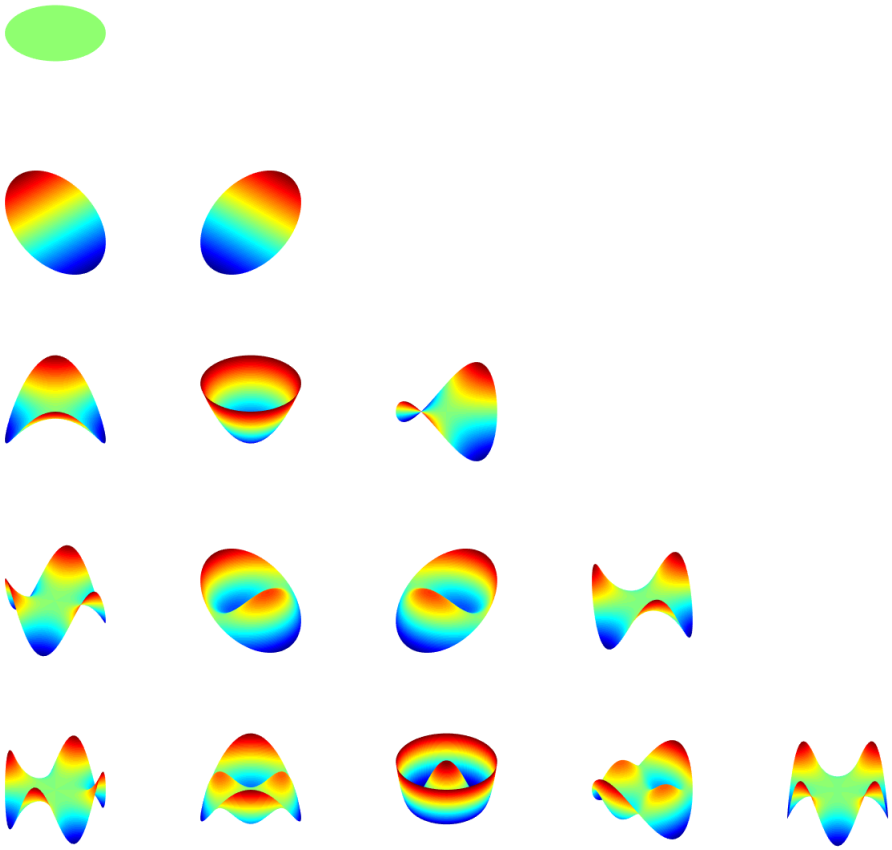

Figure 4.4: All Zernike polynomials up to $n = 4$. From top to bottom we have $n = 0, 1, 2, 3, 4$. From left to right we have $m = -n, -n+2, \ldots, n-2, n$. The colour indicates the height of the polynomial. Note that the polynomials are rotated 45° around the z axis for clarity.

Another way of displaying the polynomials is from the top view.

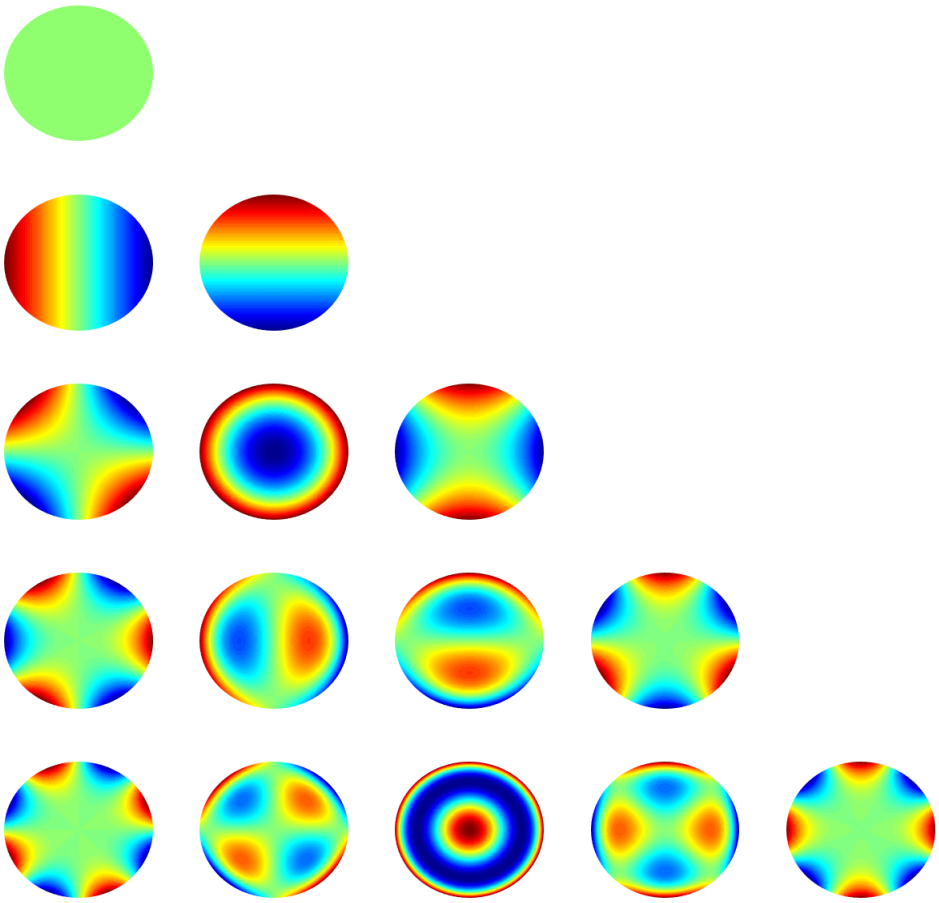

Figure 4.5: All Zernike polynomials up to $n = 4$. From top to bottom we have $n = 0, 1, 2, 3, 4$. From left to right we have $m = -n, -n+2, ..., n-2, n$. The colour indicates the height of the polynomial. Note that the polynomials are not rotated

We observe a few things. First of all, for $n = 0$, the surface is flat. This is the average offset from the x, y plane of a function $f(x, y, z)$. The Zernike parts for $n \neq 0$, the average offset for the x, y plane is zero. For different values of m, we recognise m periods on the boundaries. For higher value of m, the more steep the derivative both in the r and θ direction becomes. That means that for smooth surfaces, only the first terms of the Zernike polynomials are needed to describe it.

4.3. Finding expression for coefficients

We have found that the Zernike polynomials can describe 2D surfaces on a unit disc. We shall now describe how to find the coefficients in equation 4.1 in order to describe the profile of a surface. Since we have a set of complete eigenvectors, we can safely say

$$f(r,\theta) \sim \sum_{n,m} C_n^m Z_n^m(r,\theta)$$

The symbol ~denotes convergence in the L^2 norm. That means that the function f and its polynomial representation can only differ on finitely many points with measure zero in the Lebesgue sense. When we assume that $f(r,\theta)$ is smooth enough, we can replace ~with a = and have point wise convergence. This is a safe assumption because we are dealing with lenses. If the surface becomes rougher than the critical angle of a material, there is total reflection and our lens would not work anymore. We multiply the above equation with

a eigenfunction and integrate over the relevant surface area[1] and obtain

$$\begin{aligned}\int_{\odot} f(r,\theta) Z_{n'}^{m'}(r,\theta) r \,\mathrm{d}a &= \int_{\odot} \sum_{n,m} C_n^m Z_n^m(r,\theta) Z_{n'}^{m'}(r,\theta) r \,\mathrm{d}a \\ &= \sum_{n,m} C_n^m \int_{\odot} Z_n^m(r,\theta) Z_{n'}^{m'}(r,\theta) r \,\mathrm{d}a \\ &= \sum_{n,m} C_n^m h_{n'}^{m'} \delta_{nn'} \delta_{mm'} \\ &= h_{n'}^{m'} C_{n'}^{m'}\end{aligned}$$

Where we employed the linearity of the integral, orthogonality of the Zernike polynomials - where h_n^m denotes the orthogonality constant - and find an explicit expression for the coefficients.The $\odot$ denotes the unit disc - the area over which the Zernike polynomials are orthonormal.

$$C_{n'}^{m'} = \frac{2(n+1)}{(1+\delta_{m0})\pi} \int_{\odot} f(r,\theta) Z_{n'}^{m'}(r,\theta) r \,\mathrm{d}a \tag{4.2}$$

Calculating coefficients

The expression involves an integral over the the lens. In general, one does not have continuous surface over which the integral can be calculated nicely, but a finite amount of datapoints. For example the SMS method described earlier gives us a finite set of points that are spaced apart, but also a lens or intensity distribution is often given in 'raw data'. Therefore, when calculating the integral directly via a numerical algorithm, like the trapezoid method, this will result in large errors, especially when the distance between datapoints is large. This can be detrimental since the higher order terms have more zeros, leading to over fitting and other numerical shenanigans. Fortunately, we assumed that the original surface f was smooth, so we can use spline interpolation. I will not go into the details of spline interpolation, but it suffices to know that it returns a smooth (second order continuous derivative) piecewise polynomial. We use the lens found in the appendix as an example to show the convergence of the spline interpolation.

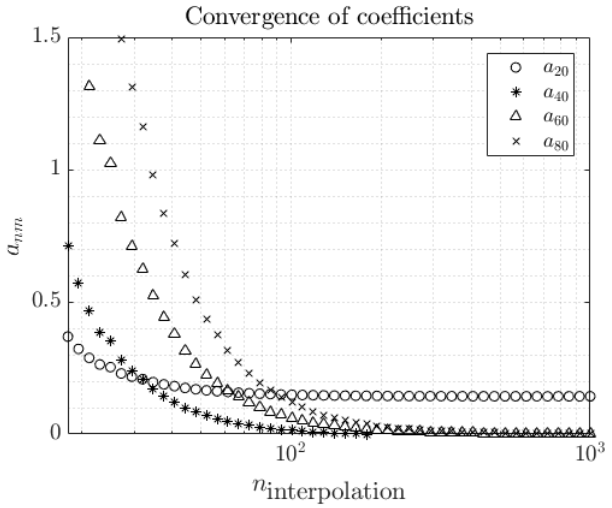

Figure 4.6: Number of points used for interpolation versus the value of the coefficients plotted on a logarithmic scale.

We can clearly see the algorithm smoothly converges to certain values. As expected we see that the higher order terms converge slower and that higher order terms have smaller values then lower order terms when the number of interpolated terms is high enough. We see that we need at least 700 interpolation points for this lens. Since we have an explicit expression for the coefficients, the computational costs for finding these

[1] This technique is known as Fourier's trick since he did it with his Fourier series. This is commonly used in solving partial differential equations, specifically the Poisson equation.

coefficients is extremely low. That's why it's recommended to check the convergence of the coefficients with a plot like above to check the validity. We can plot a mesh of the lens to see the results.

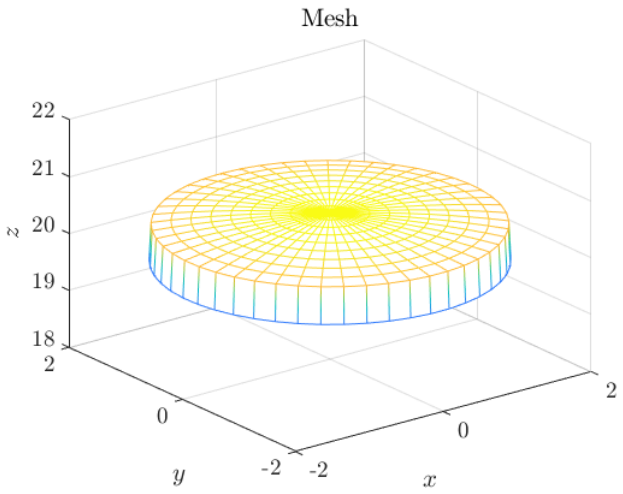

Figure 4.7: Mesh of the completed SMS method after fitting with the Zernike polynomials. The colormap is not displayed, but the height changes with colour.

The figure we get is made by a linear combination of the Zernike polynomials with the coefficients as weight. In the results section of this report we will look at more cases and see the strengths and weaknesses of the fit more clearly.

5 Results

This chapter combines the ideas found in chapter 3 and 4 to solve the problem set out in chapter 2. The first part of this chapter will develop solutions to the problem, whereas the second part will discuss the implementation of these solutions.

5.1. Semi-analytic solution to Laplacian magic window

We try to find a solution to the Laplacian magic window problem. For simplicity we regard the radially symmetric case first, so we work in cylinder coordinates and θ is constant. The $z-$axis is in the direction of the optical axis and r denotes the radius of the wavefront. The intensity is, in short field approximation, then given by:

$$I(z,r) = \frac{1}{1+(n-1)z\triangle h(r)}$$

where $h(r)$ is the height of the surface of the lens in the z direction and n the refractive index of the material. $\triangle$ denotes the Laplacian operator. This can be linearised to

$$I(z,r) = 1-(n-1)z\triangle h(r) \tag{5.1}$$

Under the assumption that we are in the short field. Because the method only works in the short field, this approximation is reasonable. In section 5.4 the difference between these methods will be discussed more in depth.

We take a look at the direct problem: we know the surface h, what is the intensity at z? Therefore we calculate the Laplacian of h. Since the problem is radially symmetric we write h in Zernike polynomials.

$$h(r) = \sum_{n,m} C_n^m R_n^m(r) \tag{5.2}$$

where C_n^m are the Fourier (more accurately: Zernike) coefficients and $R_n^m(r)$ is the radial function of the Zernike polynomials. Note that n walks from 0 to infinity and m from $-n$ to n in steps of 2. The double summation and limits make things untidy so we stick to the single sum notation, but remember this is actually a double sum with different limits. Since the Laplacian is a linear operator we can calculate the Laplacian of a single radial function $R_n^m(r)$ without loss of generality. In chapter 3 we have done exactly that: in two ways we have found Laplacian. The first attempt is by myself, and the second one is found in literature.

5.1.1. Novel method

In chapter 3 the following expression was derived.

$$\begin{aligned}\triangle R_n^m(r) = \frac{1}{r^2(1-r^2)^2}\Big[& \\ & R_n^m(r)(r^4(n+2)^2+2r^2(m(n+3)+n+2)+m^2) \\ & R_{n+1}^{m+1}(r)r(n+m+2)(r^2(2n+6)+2m+2) \\ & R_{n+2}^{m+2}(r)r^2(n+m+2)(n+m+4) \qquad \Big] \\ = & A(r)R_n^m(r)+B(r)R_{n+1}^{m+1}(r)+D(r)R_{n+2}^{m+2}(r)\end{aligned}$$

where $A(r)$, $B(r)$, and $D(r)$ are elementary functions, but not polynomials. The next subsection will show that we have indeed made no algebra errors. We return to the equation above and notice a problem. The coefficients A, B, and C are a function of r. That means we cannot use Fourier's trick directly to solve the inverse problem. I shall show where this goes wrong. Let us return to expression 5.1, use equation 5.2 and fill in the results we have just found.

$$I(z,r) = 1-(n-1)z\triangle\sum_{n,m}C_n^m R_n^m(r) \tag{5.3}$$

$$= 1-(n-1)z\sum_{n,m}C_n^m\triangle R_n^m(r) \tag{5.4}$$

$$= 1-(n-1)z\sum_{n,m}C_n^m\left(A(r)R_n^m(r)+B(r)R_{n+1}^{m+1}(r)+D(r)R_{n+2}^{m+2}(r)\right) \tag{5.5}$$

Now we write the intensity as a Zernike decomposition and use Fourier's trick

$$\sum_{n,m}E_n^m(z)R_n^m(r) = 1-(n-1)z\sum_{n,m}C_n^m\left(A(r)R_n^m(r)+B(r)R_{n+1}^{m+1}(r)+D(r)R_{n+2}^{m+2}(r)\right) \tag{5.6}$$

$$\int_0^1\sum_{n,m}E_n^m(z)R_n^m(r)R_{n'}^{m'}(r)r\,\mathrm{d}r = \int_0^1 R_{n'}^{m'}(r)r\,\mathrm{d}r - \int_0^1(n-1)z\sum_{n,m}C_n^m\left(A(r)R_n^m(r)+B(r)R_{n+1}^{m+1}(r)+D(r)R_{n+2}^{m+2}(r)\right)R_{n'}^{m'}(r)r\,\mathrm{d}r \tag{5.7}$$

$$E_{n'}^{m'}(z) = \int_0^1 R_{n'}^{m'}(r)r\,\mathrm{d}r - (n-1)z\int_0^1\sum_{n,m}C_n^m\left(A(r)R_n^m(r)+B(r)R_{n+1}^{m+1}(r)+D(r)R_{n+2}^{m+2}(r)\right)R_{n'}^{m'}(r)r\,\mathrm{d}r \tag{5.8}$$

$$= \int_0^1 R_{n'}^{m'}(r)r\,\mathrm{d}r - (n-1)z\sum_{n,m}C_n^m\int_0^1\left(A(r)R_n^m(r)+B(r)R_{n+1}^{m+1}(r)+D(r)R_{n+2}^{m+2}(r)\right)R_{n'}^{m'}(r)r\,\mathrm{d}r \tag{5.9}$$

This cannot be solved easily[1]. The next chapter will explain more carefully why this cannot be solved and will discuss several attempts at solves this equation. In conclusion this means that my method meets a dead end here. However, in literature a way has been found to circumvent this problem and this will be discussed next.

5.1.2. Janssen

We have found an expression of the Laplacian and inverse Laplacian of the Zernike polynomials. These can be used to our advantage. First we try to solve the direct problem. We introduce the notation

$$i(j)k = i, i+j, i+2j, ..., k-j, k \tag{5.10}$$

[1] Integration by parts cannot be used easily since the functions are not polynomials

where i, j and k are integers such that $i-k\equiv 0 \mod j$. Let n_r denote the refractive index to avoid confusion. Let h_n^m denote the orthogonality constant, then we deduce

$$
\begin{aligned}
I(z,r) &= 1-(n-1)z\triangle h(r)\\
\sum_{n,m} C_n^m(z)Z_n^m(r,\theta) &= 1-(n_r-1)z\triangle\left(\sum_{n,m} D_n^m Z_n^m(r,\theta)\right)\\
\sum_{n,m} C_n^m(z)Z_n^m(r,\theta) &= 1-(n_r-1)z\sum_{n,m} D_n^m\triangle\left(Z_n^m(r,\theta)\right)\\
\sum_{n,m} C_n^m(z)Z_n^m(r,\theta) &= 1-(n_r-1)z\sum_{n,m} D_n^m\sum_{s=|m|(2)(n-2)}(s+1)(n+s+2)(n-s)Z_s^m(r,\theta)\\
\int_{\odot}\sum_{n,m} C_n^m(z)Z_n^m(r,\theta)Z_{n'}^{m'}(r,\theta)r\,\mathrm{d}\tau &= \int_{\odot} Z_{n'}^{m'}(r,\theta)r\,\mathrm{d}\tau\\
&\quad -\int_{\odot}(n_r-1)z\sum_{n,m} D_n^m\sum_{s=|m|(2)(n-2)}(s+1)(n+s+2)(n-s)Z_s^m(r,\theta)Z_{n'}^{m'}(r,\theta)r\,\mathrm{d}\tau\\
\sum_{n,m} C_n^m(z)\int_{\odot} Z_n^m(r,\theta)Z_{n'}^{m'}(r,\theta)r\,\mathrm{d}\tau &= \int_{\odot} Z_0^0(r,\theta)Z_{n'}^{m'}(r,\theta)r\,\mathrm{d}\tau\\
&\quad -(n_r-1)z\sum_{n,m} D_n^m\sum_{s=|m|(2)(n-2)}(s+1)(n+s+2)(n-s)\int_{\odot} Z_s^m(r,\theta)Z_{n'}^{m'}(r,\theta)r\,\mathrm{d}\tau\\
C_{n'}^{m'}(z)h_{n'}^{m'} &= h_0^0\delta_{0n'}\delta_{0m'}-(n_r-1)z\sum_{n,m} D_n^m\sum_{s=|m|(2)(n-2)}(s+1)(n+s+2)(n-s)h_{n'}^{m'}\delta_{sn'}\delta_{mm'}\\
C_{n'}^{m'}(z)h_{n'}^{m'} &= h_0^0\delta_{0n'}\delta_{0m'}-(n_r-1)z\sum_{n} D_n^{m'}\sum_{s=|m'|(2)(n-2)}(s+1)(n+s+2)(n-s)h_{n'}^{m'}\delta_{sn'}\\
C_{n'}^{m'}(z) &= \delta_{0n'}\delta_{0m'}-\frac{2(n'+1)(n_r-1)z}{(1+\delta_{m0})\pi}\sum_{n} D_n^{m'}\sum_{s=|m'|(2)(n-2)}(s+1)(n+s+2)(n-s)h_{n'}^{m'}\delta_{sn'}\\
C_{n'}^{m'}(z) &= \delta_{0n'}\delta_{0m'}-(n_r-1)z\sum_{n} T_{n'\in|m'|(2)D_n^{m'}(n-2)}(s+1)(n+s+2)(n-s)
\end{aligned}
$$

Where we define $T_{n'\in|m|(2)(n-2)}$ to be equal to 1 if $n'\in|m|(2)(n-2)$ and 0 otherwise. This means we have found an explicit expression for Zernike coefficients of the intensity as a function of the Zernike coefficients of the surface. Note that all sums become finite if the lens is given as a finite sum of Zernike coefficients. This is exactly the expression we desire. Then we look at the inverse problem. We use the inverse Laplacian to obtain.

$$
\begin{aligned}
1-(n_r-1)z\triangle h(r) &= I(z,r)\\
\triangle h(r) &= \frac{1}{(n_r-1)z}I(z,r)-\frac{1}{(n_r-1)z}\\
h(r) &= \triangle^{-1}\left(\frac{1}{(n_r-1)z}I(z,r)-\frac{1}{(n_r-1)z}\right)\\
h(r) &= \triangle^{-1}\left(\frac{1}{(n_r-1)z}\sum_{n,m} C_n^m Z_n^m(r,\theta)\right)-\triangle^{-1}\left(\frac{1}{(n_r-1)z}\right)\\
h(r) &= \frac{1}{(n_r-1)z}\sum_{n,m} C_n^m\triangle^{-1}\left(Z_n^m(r,\theta)\right)-\frac{1}{(n_r-1)z}\triangle^{-1}1\\
h(r) &= \frac{1}{(n_r-1)z}\sum_{n,m} C_n^m\left(\frac{1}{4(n+1)(n+2)}Z_{n+2}^m(r,\theta)-\frac{1}{2n(n+2)}Z_n^m(r,\theta)+\frac{1}{4n(n+1)}Z_{n-2}^m(r,\theta)\right)\\
&\quad -\frac{1}{8(n_r-1)z}Z_2^0(r,\theta)
\end{aligned}
$$

Here we have used that the inverse Laplacian is a linear operator. We present a proof in theorem 5.1.1 of the more general case. The coefficients can then easily be found using Fourier's trick again

$$\begin{aligned}
\sum_{n,m} D_n^m(z) Z_n^m(r,\theta) &= \frac{1}{(n_r-1)z}\sum_{n,m} C_n^m \left(\frac{1}{4(n+1)(n+2)} Z_{n+2}^m(r,\theta) - \frac{1}{2n(n+2)} Z_n^m(r,\theta) + \frac{1}{4n(n_r+1)} Z_{n-2}^m(r,\theta)\right) \\
&\quad - \frac{1}{8(n_r-1)z} Z_2^0(r,\theta) \\
D_{n'}^{m'}(z) h_{n'}^{m'} &= \int \frac{1}{(n_r-1)z}\sum_{n,m} C_n^m \left(\frac{1}{4(n+1)(n+2)} Z_{n+2}^m(r,\theta) - \frac{1}{2n(n+2)} Z_n^m(r,\theta)\right) Z_{n'}^{m'}(r,\theta) r \,\mathrm{d}\, a \\
&\quad + \int \frac{1}{(n_r-1)z}\sum_{n,m} C_n^m \frac{1}{4n(n+1)} Z_{n-2}^m(r,\theta) Z_{n'}^{m'}(r,\theta) r \,\mathrm{d}\, a - \int \frac{1}{8(n_r-1)z} Z_2^0(r,\theta) Z_{n'}^{m'}(r,\theta) r \,\mathrm{d}\, a \\
D_{n'}^{m'}(z) h_{n'}^{m'} &= \frac{1}{(n_r-1)z}\sum_{n,m} C_n^m \left(\frac{1}{4(n+1)(n+2)} \delta_{(n+2)n'}\delta_{mm'} h_{n'}^{m'} - \frac{1}{2n(n+2)} \delta_{nn'}\delta_{mm'} h_{n'}^{m'}\right) \\
&\quad + \frac{1}{(n_r-1)z}\sum_{n,m} C_n^m \frac{1}{4n(n+1)} \delta_{(n-2)n'}\delta_{mm'} h_{n'}^{m'} - \frac{1}{8(n_r-1)z} h_{n'}^{m'} \delta_{2n'}\delta_{0m'} \\
D_{n'}^{m'}(z) h_{n'}^{m'} &= \frac{1}{(n_r-1)z}\left(C_{n'+2}^{m'} \frac{1}{4(n'+3)(n'+4)} h_{n'+2}^{m'} - C_{n'}^{m'} \frac{1}{2n'(n'+2)} h_{n'}^{m'} + C_{n'-2}^{m'} \frac{1}{4(n'-1)(n'-2)} h_{n'-2}^{m'}\right) \\
&\quad - \frac{1}{8(n_r-1)z} h_2^0 \delta_{2n'}\delta_{0m'} \\
D_{n'}^{m'}(z) &= \frac{1}{(n_r-1)z}\left(C_{n'+2}^{m'} \frac{1}{4(n'+3)(n'+4)} \frac{n'+1}{n'+3} - C_{n'}^{m'} \frac{1}{2n'(n'+2)} + C_{n'-2}^{m'} \frac{1}{4(n'-1)(n'-2)} \frac{n'+1}{n'-1}\right) \\
&\quad - \frac{1}{8(n_r-1)z} \delta_{2n'}\delta_{0m'} \\
D_{n'}^{m'}(z) &= \frac{1}{(n_r-1)z}\left(\frac{n'+1}{4(n'+3)^2(n'+4)} C_{n'+2}^{m'} - \frac{1}{2n'(n'+2)} C_{n'}^{m'} + \frac{n'+1}{4(n'-1)^2(n'-2)} C_{n'-2}^{m'} + \frac{\delta_{2n'}\delta_{0m'}}{8}\right)
\end{aligned}$$

A careful reader will notice that some coefficients will not be defined since a 'divide by zero' will occur. Furthermore we can have negative values of n in Z_n^m. These problems can easily be solved by setting all of these coefficients to zero since they don't represent physical values.

Theorem 5.1.1. *Let $f : A \to B$ be a linear function and $g = f^{-1}$. Then, if g exists, g is a linear function.*

Proof. Assume that g exists, then first all we prove that $g(av) = ag(v)$ for all constants[2] $a \in \mathbb{R}$ and $v \in B$. Let $x \in A$ such that $f(x) = v$. Then we find $g(av) = g(af(x)) = g(f(ax)) = ax = ag(v)$. Secondly we prove $g(v+w) = g(v) + g(w)$ for all $v, w \in B$. Let $x, y \in B$ such that $f(x) = v$, $f(y) = w$. Then $g(v+w) = g(f(x) + f(y)) = g(f(x+y)) = x + y = g(v) + g(w)$. □

Since a linear operator is defined as a linear map between two vector spaces and we know that the inverse operator is the inverse map, the inverse of the linear operator is again a linear operator. Since the Laplacian is linear, then so must the inverse Laplacian be linear.

[2] It should be noted that the constant a is chosen to be a member of $\mathbb{R}$ because all constants used in this report are indeed real. In principle this is an arbitrary choice, as the proof is easily generalised by choosing a constant from any ordered field $\mathbb{F}$.

A second way to find the surface is similar to the way my own method was supposed to work.

$$
\begin{aligned}
1-(n-1)z\triangle h(r) &= I(z,r)\\
\triangle h(r) &= \frac{1}{(n_r-1)z}I(z,r)-\frac{1}{(n_r-1)z}\\
\triangle\left(\sum_{n,m}C_n^m Z_n^m(r,\theta)\right) &= \frac{1}{(n_r-1)z}\sum_{n,m}D_n^m Z_n^m(r,\theta)-\frac{1}{(n_r-1)z}\\
\sum_{n,m}C_n^m\sum_{s=|m|(2)(n-2)}(s+1)(n+s+2)(n-s)Z_s^m(r,\theta)) &= \frac{1}{(n_r-1)z}\sum_{n,m}D_n^m Z_n^m(r,\theta)-\frac{1}{(n-1)z}\\
\int\sum_{n,m}C_n^m\sum_{s=|m|(2)(n-2)}(s+1)(n+s+2)(n-s)Z_s^m(r,\theta))Z_{n'}^{m'}(r,\theta))r\,\mathrm{d}\tau &= \int\frac{1}{(n_r-1)z}\sum_{n,m}D_n^m Z_n^m(r,\theta)Z_{n'}^{m'}r\,\mathrm{d}\tau\\
&\quad-\int\frac{1}{(n_r-1)z}Z_{n'}^{m'}r\,\mathrm{d}\tau\\
\sum_{s=|m|(2)(n-2)}(s+1)(n+s+2)(n-s)\sum_{n,m}C_n^m\int Z_s^m(r,\theta))Z_{n'}^{m'}(r,\theta))r\,\mathrm{d}\tau &= \frac{1}{(n_r-1)z}\sum_{n,m}D_n^m\int Z_n^m(r,\theta)Z_{n'}^{m'}r\,\mathrm{d}\tau\\
&\quad-\frac{1}{(n_r-1)z}\int Z_0^0(r,\theta)Z_{n'}^{m'}r\,\mathrm{d}\tau\\
\sum_{n,m}C_n^m\sum_{s=|m|(2)(n-2)}(s+1)(n+s+2)(n-s)h_{n'}^{m'}\delta_{sn'}\delta_{mm'} &= \frac{1}{(n_r-1)z}\left(\sum_{n,m}D_n^m h_{n'}^{m'}\delta_{nn'}\delta_{mm'}-h_0^0\delta_{0n'}\delta_{0m'}\right)\\
\sum_{n}C_n^{m'}\sum_{s=|m'|(2)(n-2)}(s+1)(n+s+2)(n-s)h_{n'}^{m'}\delta_{sn'} &= \frac{1}{(n_r-1)z}\left(\sum_{n,m}D_n^m h_{n'}^{m'}\delta_{nn'}\delta_{mm'}-h_0^0\delta_{0n'}\delta_{0m'}\right)\\
\sum_{n}T_{n'\in|m'|(2)(n-2)}C_n^{m'}(n'+1)(n+n'+2)(n-n')\frac{(1+\delta_{m'0})\pi}{2(n'+1)} &= \frac{\pi}{(n_r-1)z}\left(D_{n'}^{m'}\frac{1+\delta_{m'0}}{2(n'+1)}-\delta_{0n'}\delta_{0m'}\right)\\
\sum_{n}T_{n'\in|m'|(2)(n-2)}C_n^{m'}(n+n'+2)(n-n') &= \frac{1}{(n_r-1)z}\left(D_{n'}^{m'}\frac{1}{(n'+1)}-\delta_{0n'}\delta_{0m'}\right)
\end{aligned}
$$

Where we define $T_{n'\in|m|(2)(n-2)}$ to be equal to 1 if $n'\in|m|(2)(n-2)$ and 0 otherwise. In principle it is now possible to make a system of linear equations to find the coefficients C_n^m. It should be noted that this indirect method is not preferred since we already have a direct expression of the Zernike coefficients.

5.2. Zernike decomposition

A closer look will be taken at the convergence of the Zernike polynomials in this section. We will plot certain surfaces in the next figure and discuss the results.

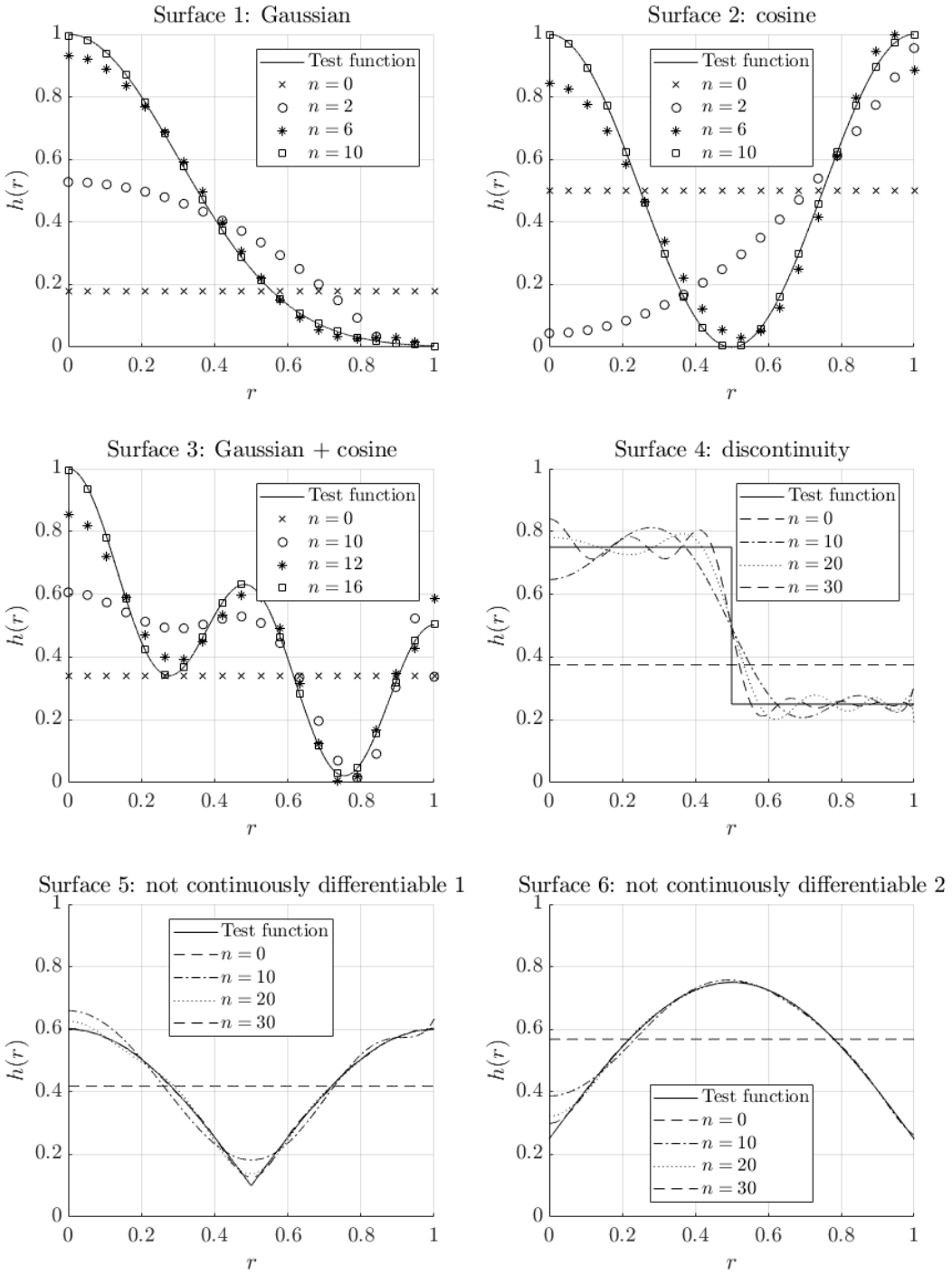

Figure 5.1: Fit of different surfaces using Zernike polynomials. The radial axis is chosen dimensionless, and the vertical axis consists of arbitrary units. The goodness of fit is discussed in the following section.

Table 5.1: Table of the test function for every surface in figure 5.1. heavi(r) denotes the heaviside step function.

Surface	Test function
1	$e^{-r^2/(2(0.3)^2)}$
2	$\frac{1}{2}+\frac{1}{2}\cos 2\pi r$
3	$\frac{1}{4}+\frac{1}{4}\cos 4\pi r+e^{-2r^2/(0.2^2)}$
4	$\frac{3}{4}-\frac{1}{2}\text{heavi}(r-\frac{1}{2})$
5	$\frac{1}{10}+\frac{1}{2}\lvert\cos(\pi r)\rvert$
6	$\frac{1}{4}+\frac{1}{2}\sin(\pi r)$

We can see from surface 1 that a function that is continuously differentiable, has low values around $r = 1$, and has a radial derivative of 0 at $r = 0$ is ideal for the Zernike polynomials to fit. Surface 1 is a Gaussian distribution, so it clearly meets these conditions. The first condition - continuously differentiable - is set because the Zernike polynomials all have this property. The second property - low values around the edge $r = 1$ - is because all the Zernike polynomials are normalised such that $R_n^m(1) = 1$. That means that in order to fit the edges correctly, the higher order terms needs to go to zero rapidly and oscillate around 0. The third condition - derivative w.r.t. r is zero at $r = 0$. A good example of the second property failing is at surface 2. Around the edge, even an order 6 fit is failing to represent the surface properly. Surface 3 is included because it is a relatively complex function, but can still be fitted properly if all 3 conditions are met sufficiently. The property of continuously differentiable can be broken 'further' by allowing discontinuities such as in surface 4. The Zernike polynomials are absolutely not fit to describe these jumping functions. When we let go of the property that a function must be continuously differentiable, but must obey the other 2 properties, we have surface 5: it can fit it approximately, but an extreme amount of terms are needed and even these cannot capture the sharpness around $r = 0.5$. The third property is counter intuitive. But we cannot have a contribution of the radial differential operator because the final Zernike polynomial consist of a rotated version of the radial function. That is why we would get a discontinuity when we differentiate the rotated version. An example of such a failing fit is given in surface 6. It should be noted that numerical errors played no role in this figures, and all coefficients converge to the values that are plotted in figure 5.1.

It should now be clear in which areas the Zernike polynomials shine and where they fail. The 3 properties a surface should have to be fitted properly are 1. continuously differentiable 2. low values around $r = 0$ and 3. zero derivative at $r = 0$.

5.3. Expression of the Laplacian

We have found multiple expressions for the Laplacian of the Zernike polynomials. In this section we will evaluate whether these are correct and how they should be implemented. This section should act as a guideline and check for implementation. In total we have found 4 expressions, which are summarised in the following table

Table 5.2: Different expressions for the Laplacian and inverse Laplacian of the Zernike polynomials discussed in this report. The numeric approach is a finite difference method.

Direct approach	$\triangle R_n^m(r)$
Summation	$\sum_{s=0}^{(n-\lvert m\rvert)/2} (-1)^s \frac{(n-s)!}{s!((n+\lvert m\rvert)/2-s)!((n-\lvert m\rvert)/2-s)!}(n-2s)^2 r^{n-2s-2}$
Novel expression	$A(r)R_n^m(r) + B(r)R_{n+1}^{m+1}(r) + D(r)R_{n+2}^{m+2}(r)$
Janssen	$\sum_{s=\lvert m\rvert(2)(n-2)} (s+1)(n+s+2)(n-s)R_s^m(r,\theta)$
Numeric	$\lim_{\mathrm{d}r\to 0} \frac{R_n^m(r+\mathrm{d}r)-2R_n^m(r)+R_n^m(r-\mathrm{d}r)}{\mathrm{d}r^2} + \frac{R_n^m(r+\mathrm{d}r)-R_n^m(r)}{\mathrm{d}r}$
Inverse approach	$\triangle^{-1} R_n^m(r)$
Janssen	$\frac{1}{4(n+1)(n+2)} R_{n+2}^m(r,\theta) - \frac{1}{2n(n+2)} R_n^m(r,\theta) + \frac{1}{4n(n+1)} R_{n-2}^m(r,\theta)$

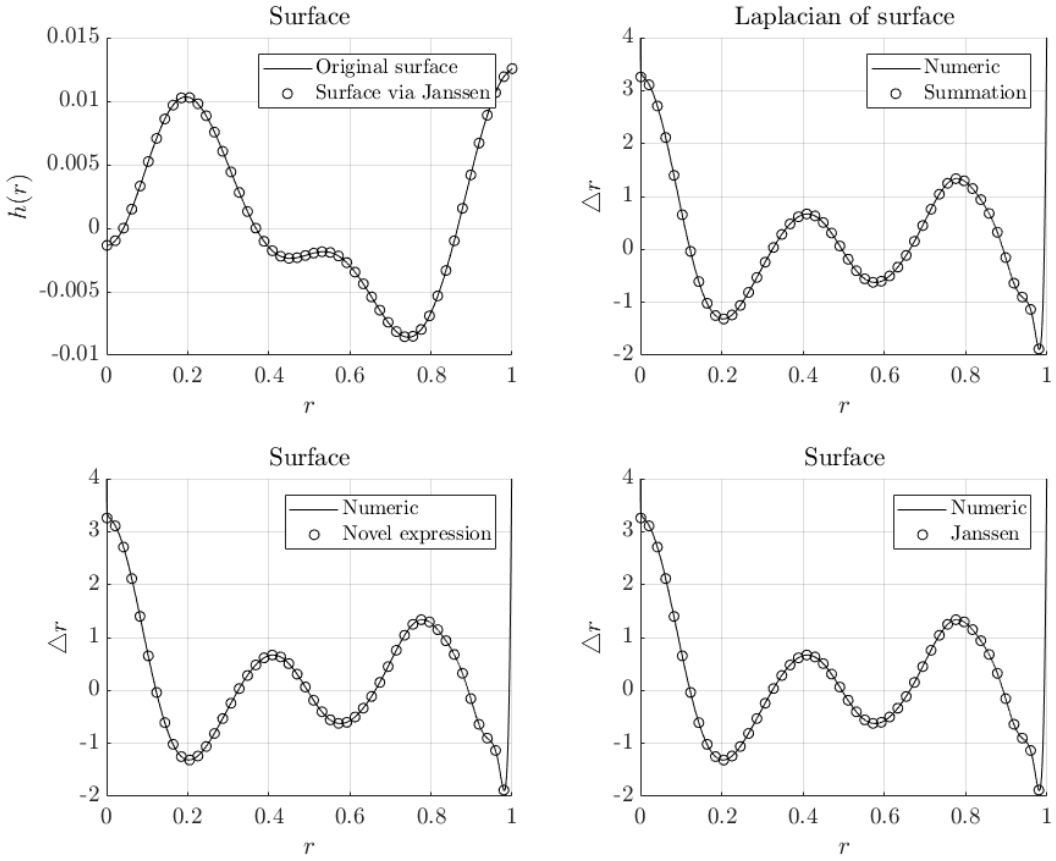

Figure 5.2: A surface[2] and the Laplacian of the surface for multiple expressions. In the upper left figure, the surface is calculated again with the inverse Laplacian via the Janssen method. The radial axis is chosen dimensionless, and the vertical axis has arbitrary units.

In the above figure a surface based on [2] is plotted and compared to the expressions found in table 5.2. First observation is that all four figures and their fits are very good as they coincide. For clarity only a few points are plotted on top of the numeric result, because the fit is so close that it cannot be distinguished. This is expected because we have found an analytic expression for them. Plotting these figures is a great tool to make sure there are no bookkeeping errors in the mathematics or implementation errors in software. In the upper left figure the inverse Laplacian is calculated by first using Janssen's method to find the Laplacian of the original surface, then calculating the inverse Laplacian via Janssen's method. The surface was chosen to

be a fit to the surface in the article of Berry[2]. This surface should be a good tool for checking because it has around 30 non zero coefficients. Because the results are so similar, one is free to use any of these methods. I recommend using the expression for Janssen. First of all these are the most general, because they also describe the whole - $m \neq 0$ - Zernike polynomials, and not only the radial part. Secondly they will be used in the inverse problem, so it is good to already have them implemented.

A special mention should be given to the implementation of the method of Janssen. This is because the summation indices and other shenanigans with the expression make it hard to implement. The following table should act as a guideline to help check solutions.

Table 5.3: Several expression calculated via the Janssen method. Based on [8]

n	m	$\triangle Z_n^m$	$\triangle^{-1} Z_n^m$
0	0	0	$\frac{1}{8} Z_2^0$
2	0	$8Z_0^0$	$-\frac{1}{16} Z_2^0 + \frac{1}{48} Z_4^0$
2	2	0	$\frac{1}{48} Z_4^2$
5	3	$80Z_3^3$	$-\frac{1}{70} Z_5^3 + \frac{1}{168} Z_7^3$
6	0	$120Z_4^0 + 120Z_2^0 + 48Z_0^0$	$\frac{1}{168} Z_4^0 - \frac{1}{96} Z_6^0 + \frac{1}{224} Z_8^0$

5.4. Direct problem

To solve the direct problem we have some options. We already know from figure 2.3 that we can use ray tracing, and the Laplacian magic window via Zernike decomposition. First we use the Laplacian magic window and calculate the intensity via the linear and non-linear expressions. We will compare this with a ray tracing algorithm. We choose 3 surfaces to solve this problem, which should be general enough and provide enough information to check solutions. These are summarised in the following table

Table 5.4: Surfaces used in the direct problem. $h(r)$ denotes the surface and $N(\mu,\sigma)$ denotes a Gaussian probability density distribution.

#	$h(r)$
1	$\frac{1}{200} N(0, \frac{3}{10})(r)$
2	$\frac{1}{2000} \cos 4\pi r$
3	Surface from figure 5.2 scaled down by factor 50

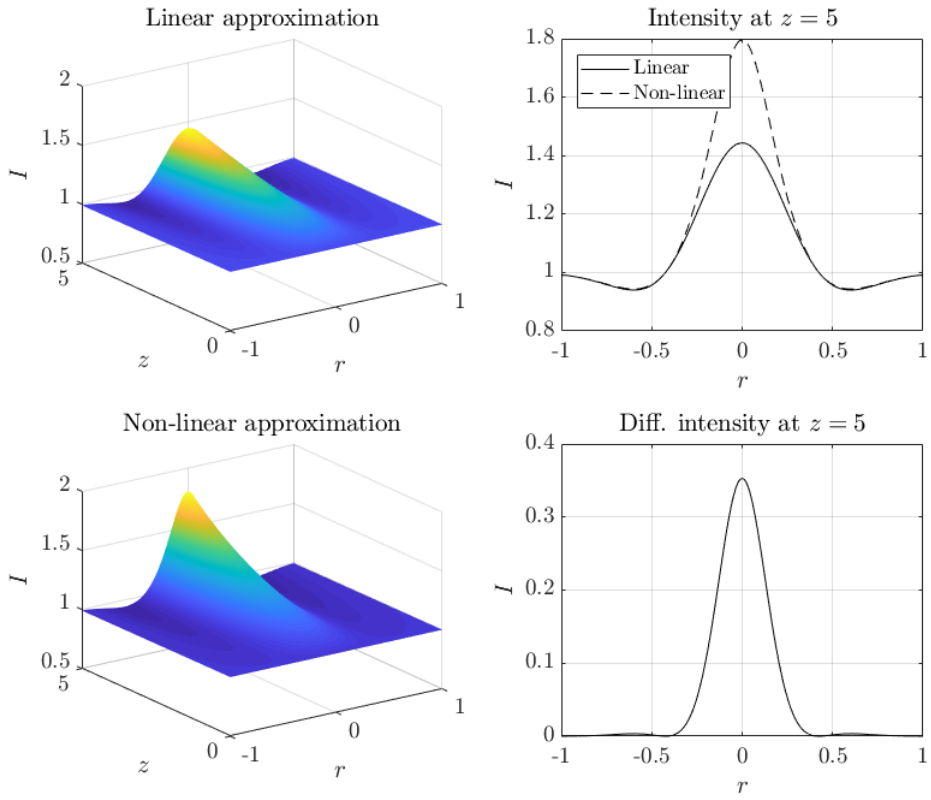

Figure 5.3: Solutions of the Laplacian magic window of surface 1 from table 5.4. Bottom right plot shows the difference in intensity between the linear and non-linear solution. All units on all axis are dimensionless or arbitrary.

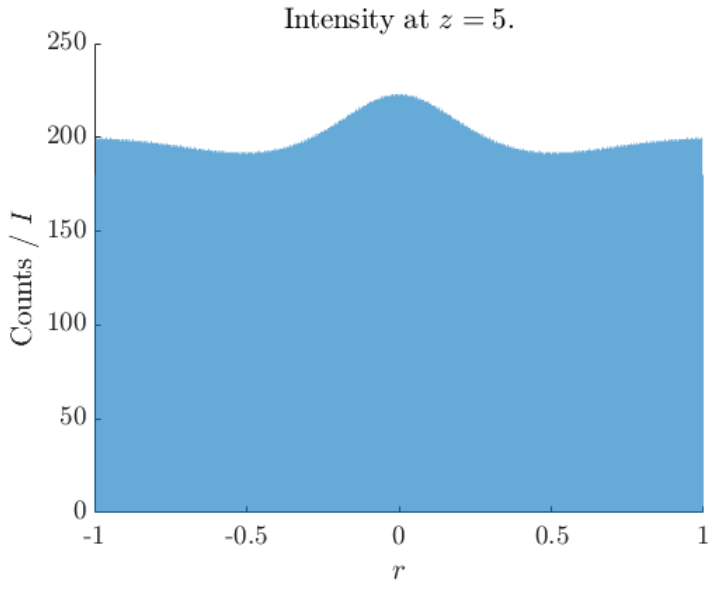

Figure 5.4: Histogram of ray tracer solution of the problem 1. The counts are proportional to the intensity.

Qualitatively the results match, but there are problems with the scaling in absolute terms and with a dependency on radius. Therefore we will not quantitatively compare the results, but discuss possible reasons why the mismatches happen in the discussion section of this report. The next implemented examples show similar behaviour.

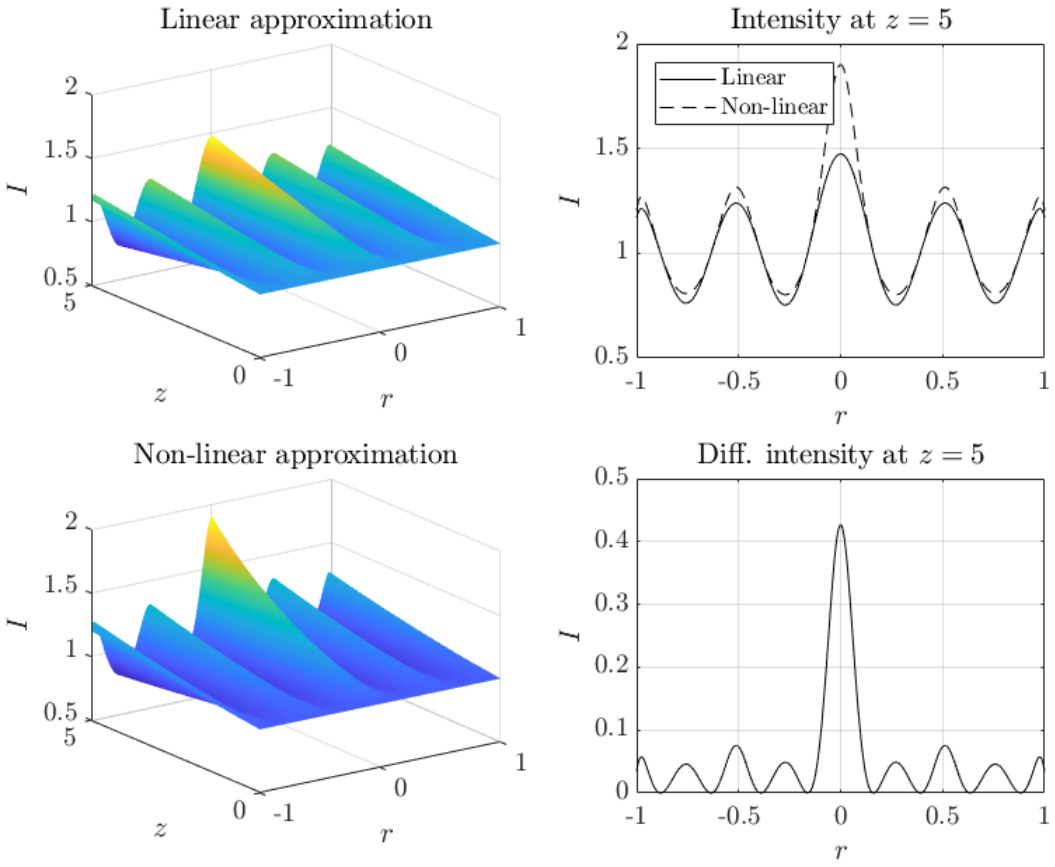

Figure 5.5: Solutions of the Laplacian magic window of surface 2 from table 5.4. Bottom right plot shows the difference in intensity between the linear and non-linear solution. All units on all axis are dimensionless or arbitrary.

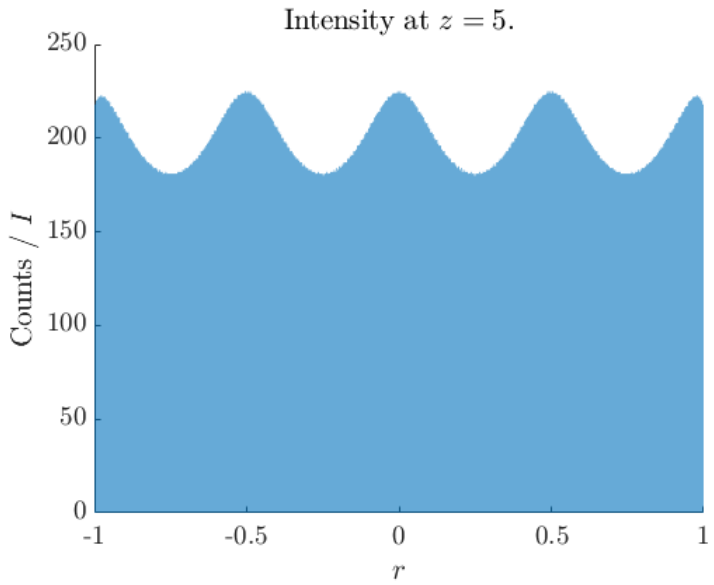

Figure 5.6: Histogram of ray tracer solution of the problem 2. The counts are proportional to the intensity.

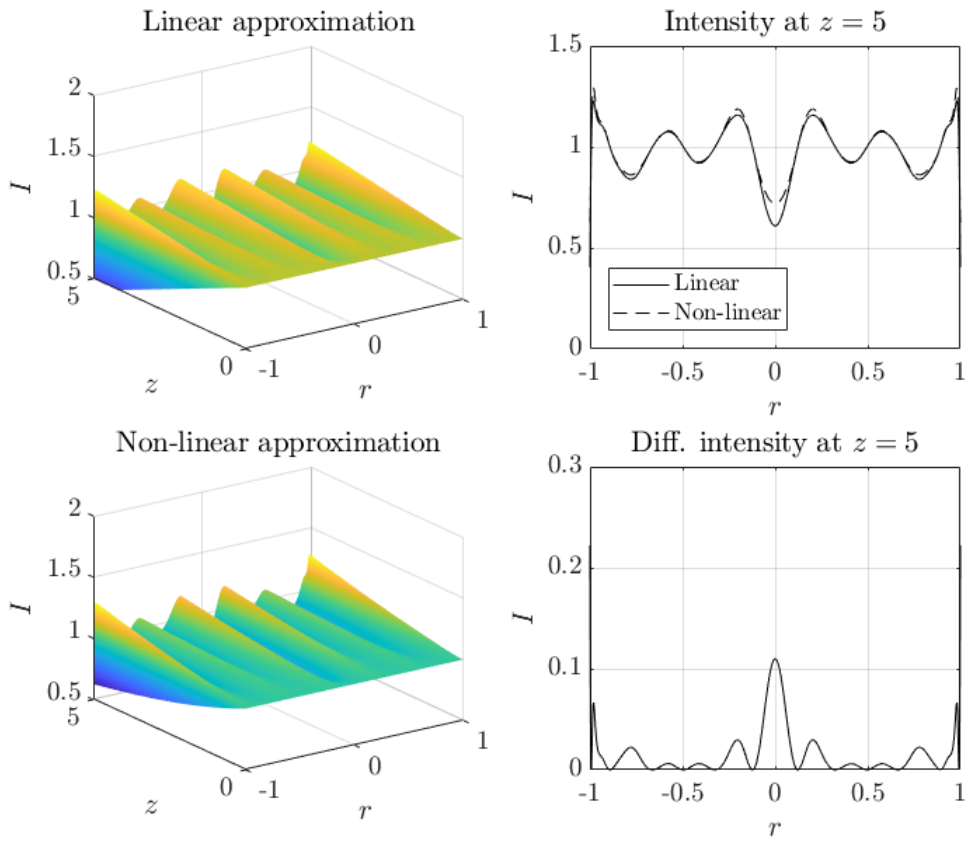

Figure 5.7: Solutions of the Laplacian magic window of surface 3 from table 5.4. Bottom right plot shows the difference in intensity between the linear and non-linear solution. All units on all axis are dimensionless or arbitrary.

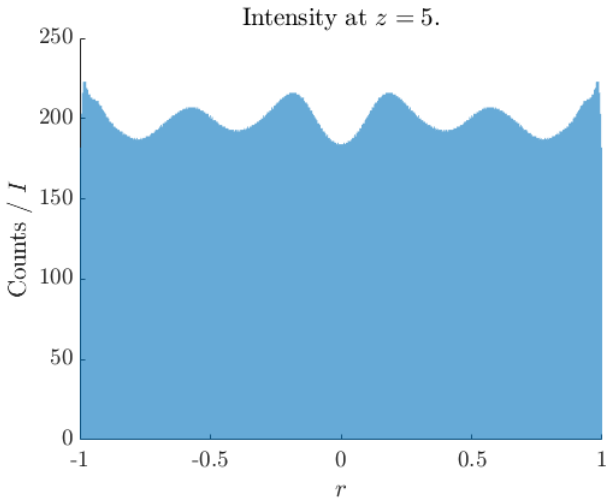

Figure 5.8: Histogram of ray tracer solution of the problem 2. The counts are proportional to the intensity.

5.5. Inverse problem: semi-analytic solution

For the inverse problem, 3 surfaces are calculated using equation 6.1. The surfaces should give an output that is given in table 5.5

Table 5.5: Surfaces used in the direct problem. $N(\mu,\sigma)$ denotes a Gaussian probability density distribution.

#	I at $z=5$
1	$1+\frac{1}{10}\cos 2\pi r$
2	$\frac{4}{5}+\frac{1}{2\sqrt{2\pi}\frac{1}{5}}N(0,\frac{1}{5})$
3	Intensity from figure 5.2

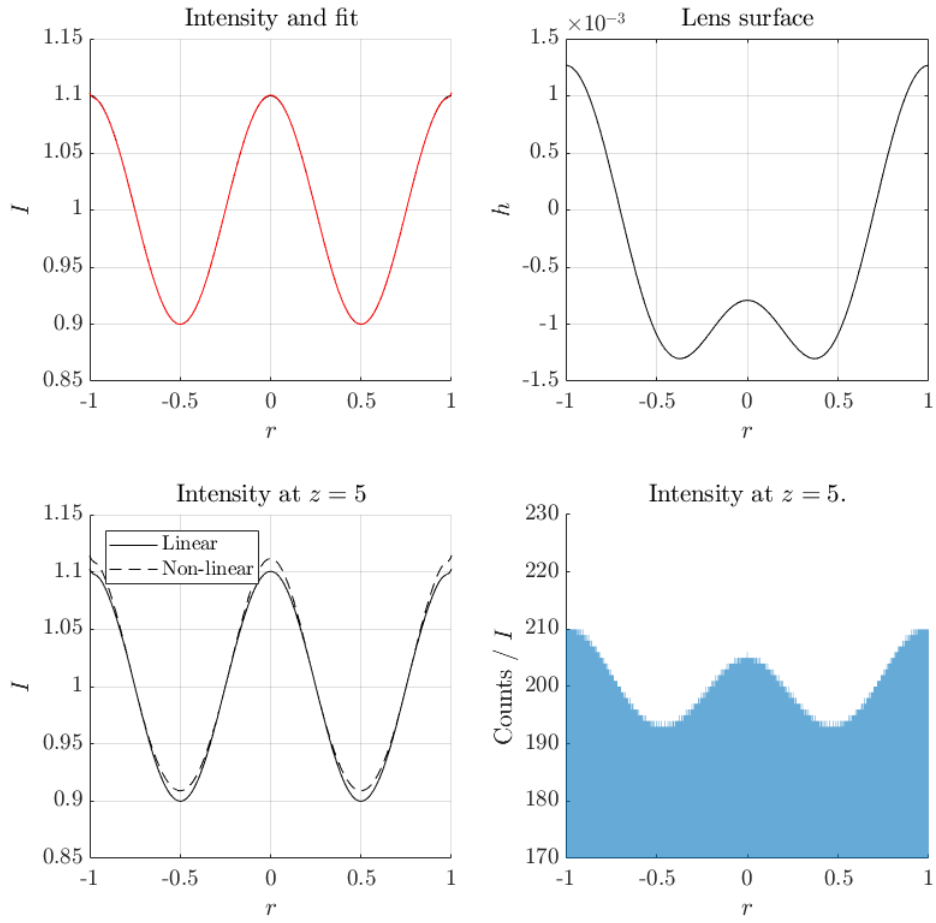

Figure 5.9: Solution to inverse problem 1. Top left figure shows the input intensity and Zernike fit at $z=5$, which almost completely overlap, in black and red respectively. Top right figure shows shows the lens as calculated via the inverse Laplacian magic window. Bottom right figure shows linear and non-linear solutions calculated by the Laplacian magic window with input the lens surface from the top right figure. Bottom right figure shows a histogram of the ray tracer solution.

The solutions again match qualitatively, but not quantitatively. This problem will again be discussed in the discussion part of the report. A good check that the implementation is correct is that the intensity output calculated from the lens by the linear Laplacian magic window method is identical to the input intensity. The intended intensity and the linear method are therefore identical. These comments are also applicable to the other surfaces calculated as can be seen in the next figures.

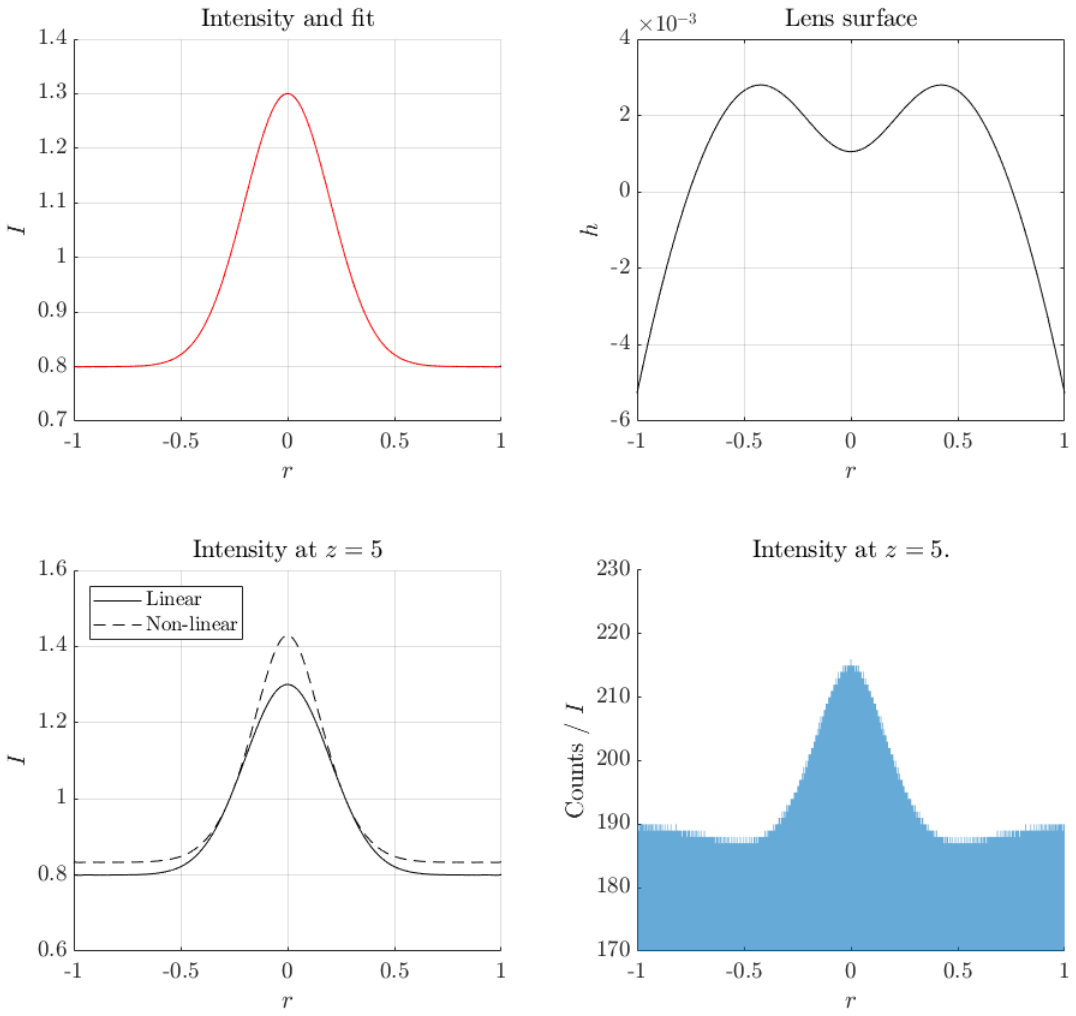

Figure 5.10: Solution to inverse problem 2. Top left figure shows the input intensity and Zernike fit at $z = 5$, which almost completely overlap, in black and red respectively. Top right figure shows shows the lens as calculated via the inverse Laplacian magic window. Bottom right figure shows linear and non-linear solutions calculated by the Laplacian magic window with input the lens surface from the top right figure. Bottom right figure shows a histogram of the ray tracer solution.

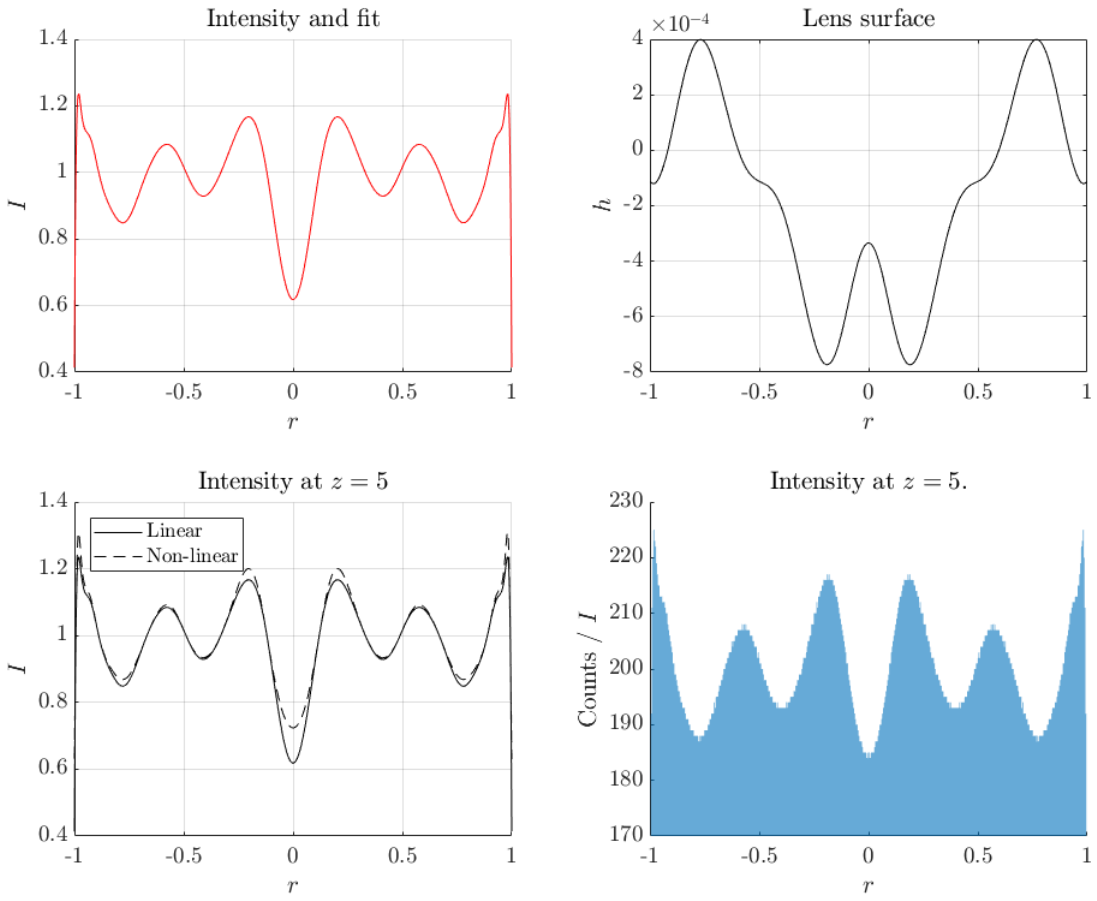

Figure 5.11: Solution to inverse problem 3. Top left figure shows the input intensity and Zernike fit at $z = 5$, which almost completely overlap, in black and red respectively. Top right figure shows shows the lens as calculated via the inverse Laplacian magic window. Bottom right figure shows linear and non-linear solutions calculated by the Laplacian magic window with input the lens surface from the top right figure. Bottom right figure shows a histogram of the ray tracer solution.

6

Discussion

In this chapter the results will be discussed and suggestions for further research are proposed.

6.1. Novel approach

The novel solution I proposed met a dead end. First I will explain more carefully why this happens, and secondly I suggest how to go forwards. To demonstrate that my solution cannot be solved further, take the $D(r)$ term [1] of the integral of the right-hand side of expression 5.9.

$$\int_0^1 D(r) R_{n+2}^{m+2}(r) R_{n'}^{m'}(r) r \,\mathrm{d}\, r = \int_0^1 \frac{(n+m+2)(n+m+4)}{(1-r^2)^2} R_{n+2}^{m+2}(r) R_{n'}^{m'}(r) r \,\mathrm{d}\, r \tag{6.1}$$

Ideally it would have to be this in the form

$$\int_0^1 R_{n+2}^{m+2}(r) R_{n'}^{m'}(r) r \,\mathrm{d}\, r = F_n^m \delta_{(n+2)n'} \delta_{(m+2)m'} \tag{6.2}$$

because this would reduce our infinite sum to a finite one and would give a finite, and explicit expression for the inverse problem. Now we are left the mercy of numerically approximating the coefficients E_n^m, and without certainty that the solution converges. This defeats the whole point of a analytic solution, it would also mean that a numerical Laplacian solver would be as fast, if not faster then first decomposing everything in Zernike polynomials, and for each coefficient, approximate 3 infinite sums. I have a few suggestions to solve this, but I cannot see how they will be fruitful.

1. Integration by parts
To solve the problem with integration by parts we need the integral expression of A, B, and D. The simplest function is D:

$$\int D(r) \,\mathrm{d}\, r = \int \frac{1}{(1-r^2)^2} \,\mathrm{d}\, r = \frac{1}{4}\left(\frac{2r}{1-r^2} - \ln(1-x) + \ln(1+x)\right)$$

This is not in any form to make the reach expression 6.2. The functions A and B are even less orderly.

2. Reduce terms.
In theorem 3.3.6 we have found

$$R_n^m(r) = \frac{1}{2(n+1)r}\left((n+m+2)R_{n+1}^{m+1} + (n-m)R_{n-1}^{m-1}\right)$$

So we can write the Laplacian in 2 terms:

$$\triangle R_n^m(r) = A'(r) R_n^m(r) + D'(r) R_{n+2}^{m+2}(r)$$

[1] We take the $D(r)$ term because it is the simplest expression of the three.

Where $A'(r)$ and $D'(r)$ are even worse expressions than A and D, so reducing the three terms to two would create the same problem as for solution 1.

3. No solution.

It could of course be that there is no analytic solution. That means my approach here meets a dead end. However literature provides us with a solution. Janssen solved the problem [8] which suggests there might be some way to solve this. For now however, it is not worth trying to solve this because no new ways to solve it have presented themselves[2], especially since Janssen already found another expression. Therefore it is suggested to use the method of Janssen.

6.2. Direct and inverse problem

The solutions of the direct and inverse problem match the ray tracing algorithm qualitatively. This is expected because the surfaces have been chosen with care. They had to meet the three conditions set out in section 5.2 in order to accurately fit the data. Secondly they seem to meet the criterion that only the short field applies i.e. no caustics. The surfaces have been chosen to be very smooth in order to meet that as can be seen in small coefficients in table 5.4 and 5.5. The ray tracer also shows that the rays do not cross. Thirdly, also the surfaces obtained in the inverse problem are very small - order 10^{-4} - compared to the optical axis, which has length 5. This means the inverse problem gives back a smooth surface as required.

The explanation that the results don't match qualitatively can be explained by two factors. It is most likely that either the ray tracing, or the Laplacian magic window is not perfect. The fault cannot be in the implementation of the Laplacian magic window, because solving the solution of the inverse problem with the linear method of the Laplacian magic gives back the exact same intensity. It could be that the linear method does not capture the non linearities accurately, but when using the non-linear expression to calculate the intensity back, the problem that the ray tracer and Laplacian magic window don't give the same result gets even worse. Therefore it is likely that the problem lies with the ray tracer. It is unlikely that the implementation of the ray tracer is incorrect, because it gives back the same qualitative results. If there were a problem with the implementation, it should other incorrect behaviour. It is most likely that the problem lies with the fact that the ray tracer is implemented in Cartesian coordinates, while the Zernike representation is implemented in polar/cylindrical coordinates. The way the tracer is implemented makes it hard to correct for this. Professional software should easily be able to handle these problems, because they can take as input Zernike coefficients as they are a standard in optics. This project is not able to use this software because of time constraints as it would take a lot of time to get to know and understand new software, and it is not guaranteed that is will yield better results.

6.3. Further research

In this section I will address the shortcomings of this report and discuss how they could be improved in the future. First of all better ray tracing software can be used to check the validity of the results of the Laplacian magic window. This should be not to hard a task for a senior optical engineer.

Secondly all of the examples used in this report are in two dimensions i.e. radially symmetric. Because this report serves mostly as a proof of concept on how a semi-analytic solution can be obtained for the main problem, it is not a big issue. Also all the mathematics is general enough to easily be expanded into three dimensions i.e. taking into account asymmetric inputs in the problem. The expressions for the direct and indirect problem are already explicitly solved for three dimensions, but implementing them was beyond the scope of this project.

Thirdly, the solutions obtained with the semi-analytic method can be compared with a numerical Laplacian solving. It would be interesting to see how they would compare in quality and computational time. It is my hypothesis that especially in three dimensions, the computational time of the inverse Laplacian would be so big, that this new approach proposed would be especially useful. This report presents a good proof of concept in order to carry out this research.

Lastly, it could be considered to put more effort into solving the novel solution as it could give an easier, and thus faster, expression than what Janssen obtained. This is no priority since already a working solution exists and the chances of solving the novel solution are slim at the moment.

[2] I have contacted Janssen, who is an expert in this field, and he also sees no way to solve this.

7

Conclusion

In this report, a semi-analytic solution to the direct and inverse problem of the Laplacian magic window is proposed and implemented in 2D. The solution works by fitting the target intensity and surface with Zernike polynomials. The fitting works since the polynomials form a complete set, but precautions need to be made for an accurate fit. In the report the relevant criteria for accurate fitting are discussed. The results of the semi-analytic agree qualitatively with the numeric results and work for complex and diverse inputs. The semi-analytic solution is preferred over a numeric solution since it greatly reduces computational time and complexity. There is some discrepancy with the numerical results, but these can be explained by the shortcomings of the numerical methods in 2D. Therefore it is suggested that further efforts should be made to more accurately compare the results obtained by the semi analytic solution. This can be done by implementing the problem in 3D, which the semi-analytic solution proposed in this report is already able to solve.

Bibliography

[1] Stegun I. A. Abramowitz, M. *Handbook of mathematical functions : With formulas, graphs, and mathematical tables*. Dover Publications, 1965. ISBN 0486612724.

[2] M V Berry. Laplacian magic windows. *Journal of Optics*, 19(6):06LT01, may 2017. doi: 10.1088/2040-8986/aa6c4e. URL https://doi.org/10.1088%2F2040-8986%2Faa6c4e.

[3] Ruben Biesheuvel. Creating a rectangular illumination pattern using the sms2d method. 2017.

[4] Julio Chaves. *Introduction to non-imaging optics*. CRC Press, Boca Raton, 2015.

[5] Bram de Greve. Reflections and refractions in ray tracing. Technical report, Stanford, 2006.

[6] Szegö Gabor. *Orthogonal Polynomials*. American Mathematical Society, Providence, Rhode Island, 4 edition, 1975.

[7] M. T. Mustafa H. Azad. Sturm-liouville theory and orthogonal functions. 2009.

[8] A. J. E. M. Janssen. Zernike expansion of derivatives and laplacians of the zernike circle polynomials. *Journal of the Optical Society of America A*, 31(7), 2014.

[9] Vasudevan Lakshminarayanan and Andre Fleck. Zernike polynomials: A guide. *Journal of Modern Optics - J MOD OPTIC*, 58:1678–1678, 04 2011.

[10] Pavel Novák, Jiří Novák, and Antonín Mikš. Fast and robust computation of cartesian derivatives of zernike polynomials. *Optics and Lasers in Engineering*, 52:7 – 12, 2014. ISSN 0143-8166. doi: https://doi.org/10.1016/j.optlaseng.2013.07.012. URL http://www.sciencedirect.com/science/article/pii/S0143816613002285.

[11] James C. Wyant. Zernikepolynomialsfortheweb.nb. Technical report, University of Arizona, 2003.

[12] James C. Wyant and Katherine Creath. *Basic Wavefront Aberration Theory for Optical Metrology*. 1998.

A

SMS2D Method

Simultaneous Multiple Surfaces

The Simultaneous Multiple Surfaces in 2 dimensions (SMS2D) method is a method to construct lenses. It is an iterative method that uses geometrical optics to find the 2 surfaces of the lens at the same time. The method described first is a method in 2 spacial dimensions. That means that the final (3-dimensional) lens will be a rotated version of the end product of the SMS2D method.
The SMS2D method can be described in 4 steps[3]

1. Find starting points
2. Find starting normals
3. Initialise first rays
4. Continue SMS chain until symmetry axis is reached

After which points on the surface of the lens are found like in figure A.1

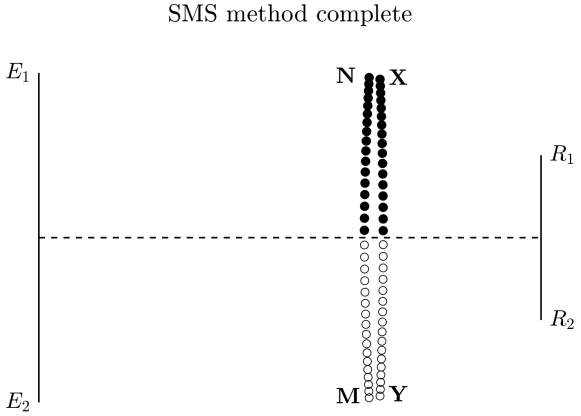

Figure A.1: A result of the SMS2D method. The entrance aperture NM and exit aperture XY can be seen as well as the emitter plane (E) and receiver plane (R). The filled dots are found by the SMS method. The empty dots are found by symmetry of the SMS method.

1. Find starting points

It is assumed that the étendue U is a known parameter. This is possible because the étendue describes the squeezing of the light. Therefore a small étendue corresponds with a small radius of the lens. Comparing

the étendue from the emitter plane $\boldsymbol{E_1E_2}$ to the entrance aperture $\boldsymbol{NM}$ and from the receiver plane $\boldsymbol{R_1R_2}$ exit aperture $\boldsymbol{XY}$ gives:

$$U = 2([\boldsymbol{N},\boldsymbol{E_1}] - [\boldsymbol{N},\boldsymbol{E_2}]) = 2([\boldsymbol{X},\boldsymbol{R_1}] - [\boldsymbol{X},\boldsymbol{R_2}]) \tag{A.1}$$

Where $\boldsymbol{N},\boldsymbol{M},\boldsymbol{X},\boldsymbol{Y}$ and $\boldsymbol{E_1},\boldsymbol{E_2},\boldsymbol{R_1},\boldsymbol{R_2}$ are defined in figure A.1 and $[\boldsymbol{P_1},\boldsymbol{P_2}]$ denotes the Euclidean distance between $\boldsymbol{P_1}$ and $\boldsymbol{P_2}$. In equation A.1 a reader can recognise the definition of a hyperbola. These 2 hyperbolas have foci $\boldsymbol{E_1},\boldsymbol{E_2}$ and $\boldsymbol{R_1},\boldsymbol{R_2}$ respectively. Because U is know, equation A.1 can be written as a parametrization[4]:

$$(x(\phi), y(\phi)) = \boldsymbol{P_1} + \frac{(\frac{U}{2}) - [\boldsymbol{P_1},\boldsymbol{P_2}]^2}{U - 2[\boldsymbol{P_1},\boldsymbol{P_2}]\cos\phi}(\cos\phi + \alpha, \sin\phi + \alpha). \tag{A.2}$$

which represent a hyperbola when $U < 2[\boldsymbol{P_1},\boldsymbol{P_2}]$ and an ellipse otherwise. For this application, a hyperbola is required and $\boldsymbol{P_1},\boldsymbol{P_2}$ are emitter endpoints $\boldsymbol{E_1},\boldsymbol{E_2}$ or $\boldsymbol{R_1},\boldsymbol{R_2}$. Let h_E and h_R denote this parabolas. This means that the points $\boldsymbol{N},\boldsymbol{X}$ should be chosen such that they are on h_E and h_R respectively. An example can be seen in figure A.2.

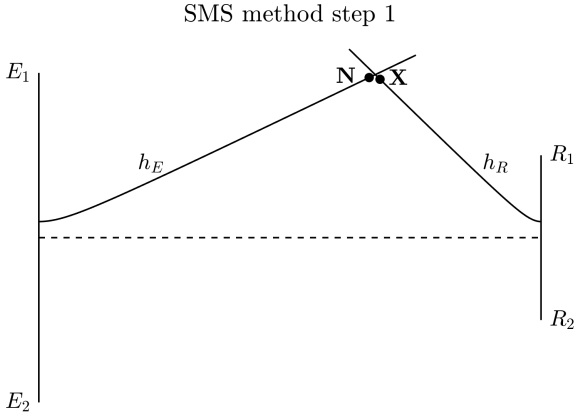

Figure A.2: First step of the SMS method. The parabolas h_E and h_R are plotted and starting points $\boldsymbol{N}$ and $\boldsymbol{X}$.

2. Find starting normals

Let the first ray be emitted from $\boldsymbol{E_2}$, refracted at $\boldsymbol{N}$ and $\boldsymbol{X}$ respectively to $\boldsymbol{R_2}$ as shown in figure A.3. Calculating the normal of the surface at $\boldsymbol{N}$ and $\boldsymbol{X}$ the surface is not a lot of work since the incoming and refracted rays are known. Let $\boldsymbol{v_i}$ and $\boldsymbol{v_r}$ denote the normalised incoming and refracted rays respectively:

$$\boldsymbol{N}: \quad \boldsymbol{v_i} = \frac{\boldsymbol{N} - \boldsymbol{E_2}}{||\boldsymbol{N} - \boldsymbol{E_2}||}, \quad \boldsymbol{v_r} = \frac{\boldsymbol{X} - \boldsymbol{N}}{||\boldsymbol{X} - \boldsymbol{N}||} \tag{A.3}$$

$$\boldsymbol{X}: \quad \boldsymbol{v_i} = \frac{\boldsymbol{X} - \boldsymbol{N}}{||\boldsymbol{X} - \boldsymbol{X}||}, \quad \boldsymbol{v_r} = \frac{\boldsymbol{R_2} - \boldsymbol{X}}{||\boldsymbol{R_2} - \boldsymbol{X}||} \tag{A.4}$$

$$\tag{A.5}$$

Where $||\boldsymbol{x}||$ denotes the L^2 norm of $\boldsymbol{x}$. Then the normal vector at the surface is

$$\boldsymbol{n} = \frac{n_i\boldsymbol{v_i} - n_r\boldsymbol{v_r}}{||n_i\boldsymbol{v_i} - n_r\boldsymbol{v_r}||} \tag{A.6}$$

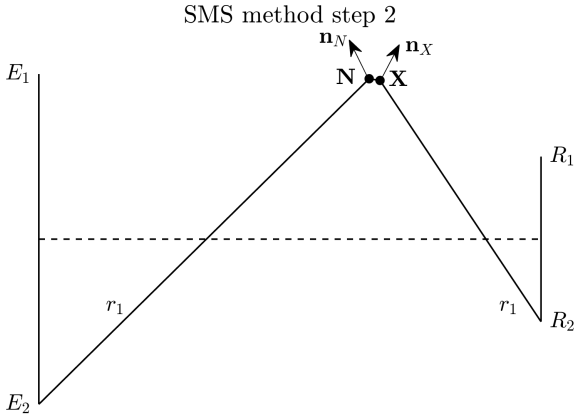

Figure A.3: Step 2 of the SMS method finds the normal vector at $\boldsymbol{N}$ and $\boldsymbol{X}$

3. Initialise first rays

In order to find second point on the second surface -$\boldsymbol{X_1}$ -, a second ray is emitted from $\boldsymbol{E_1}$ to $\boldsymbol{N}$. Because the surface normal is known, the reflected ray can be calculated as follows:

$$\boldsymbol{v_r'} = \frac{n_1}{n_2}\boldsymbol{v_i} + \left(\frac{n_1}{n_2}(\boldsymbol{v_i} \bullet \boldsymbol{n})\boldsymbol{n} - \sqrt{1 - \left(\frac{n_1}{n_2}\right)^2 (1 - (\boldsymbol{v_i} \bullet \boldsymbol{n})^2)}\right)\boldsymbol{n} \tag{A.7}$$

The derivation of equation A.7 can be found in at the end of the appendix. After normalising $\boldsymbol{v_r'}$ we can find $\boldsymbol{v_r}$.

Now that the direction of the outgoing ray is known, Fermat's principle can be used: the optical path length S between $\boldsymbol{N}$ and $\boldsymbol{R_1}$ must be the same when the path travels via $\boldsymbol{X}$ or $\boldsymbol{X_1}$. This can be precisely stated as

$$S = n[\boldsymbol{N}, \boldsymbol{X}] + [\boldsymbol{X}, \boldsymbol{R_2}] = n[\boldsymbol{N}, \boldsymbol{X_1}] + [\boldsymbol{X_1}, \boldsymbol{R_2}] \tag{A.8}$$

Then $\boldsymbol{X_1}$ can be found as follows[3]

$$\boldsymbol{X_1} = \boldsymbol{N} + C_1 \boldsymbol{v_r} \tag{A.9}$$

where

$$C_1 = \frac{C_2 - \sqrt{C_3(1 - n^2) + C_2^2}}{n^2 - 1} \tag{A.10}$$

$$C_2 = nS + (\boldsymbol{N} - \boldsymbol{R_2}) \bullet \boldsymbol{v_r} \tag{A.11}$$

$$C_3 = S^2 - ||\boldsymbol{N} - \boldsymbol{R_2}||^2 \tag{A.12}$$

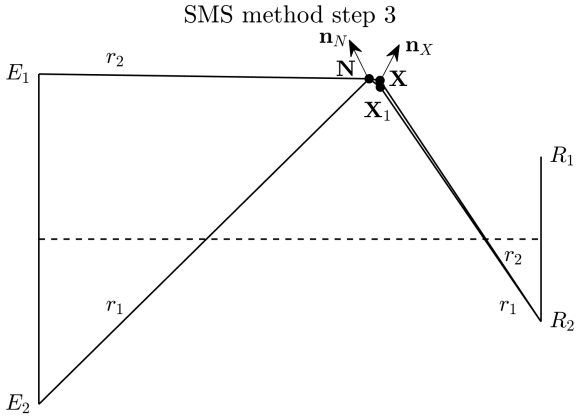

Figure A.4: Step 3 of the SMS method. A zoomed in version of this figure can be found in figure A.5

Zooming in on the relevant area around $\boldsymbol{N}$ and $\boldsymbol{X}$ gives

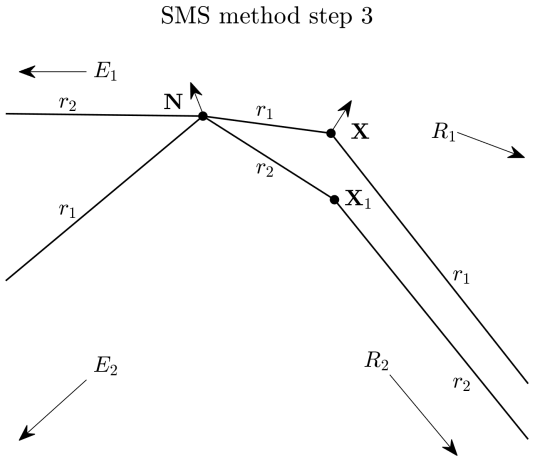

Figure A.5: Step 3 of the SMS method. The second ray r_2 is emitted from $\boldsymbol{E_1}$ and will be refracted to $\boldsymbol{R_2}$.

Now we apply the same method for the third ray to find $\boldsymbol{N_1}$. This is done by emitting a ray from $\boldsymbol{R_1}$ via $\boldsymbol{X}$ and $\boldsymbol{N_1}$ towards $\boldsymbol{E_2}$. The process is illustrated in figure A.6.

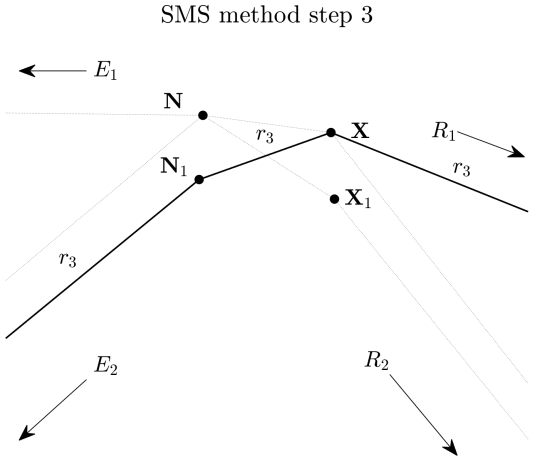

Figure A.6: Step 3 of the SMS method. The third ray r_3 is emitted from $\boldsymbol{R_1}$ and will be refracted to $\boldsymbol{E_2}$.

4. Continue SMS chain until symmetry axis is reached
The process of emitting a ray from $\boldsymbol{E_1}$ to the next point on the first surface and using Fermat's principle to find a new point on the second surface $\boldsymbol{X_i}$ and the inverse process to find N_i is repeated until the optical axis is reached. The second iteration of this method can be found in figure A.7.

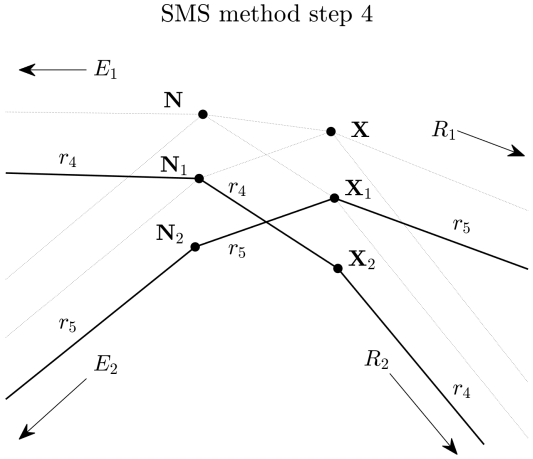

Figure A.7: The second iteration of the SMS method. This iterations finds points $\boldsymbol{X_2}$ and $\boldsymbol{N_2}$.

A first sign of the validity of the found solution the that the lens at the optical axis is orthogonal to the optical axis. This means that at least the rays from the middle of the emitter plane will be refracted to the middle of the receiver plane. More sophisticated methods can be used to check the validity of the solution, but we have already given a proof of concept, so no more attention is given to this problem.

Snell's law in vector form
In this section, a general result will be derived for the direction of the refracted ray.

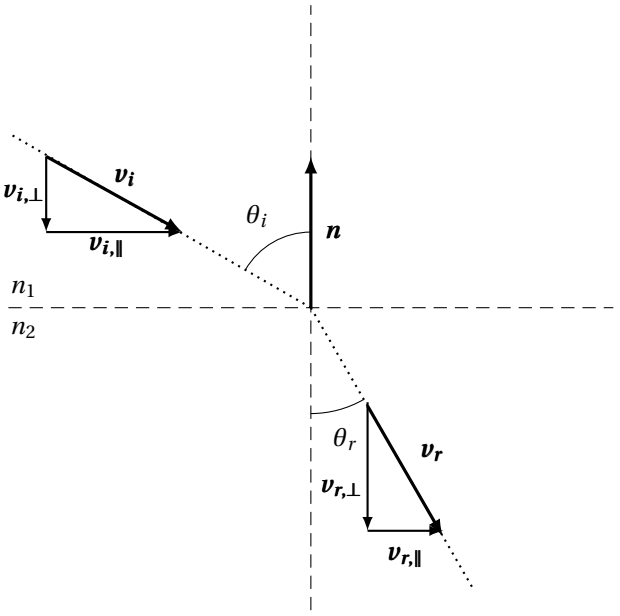

Figure A.8: Refraction of light.

First consider an incoming ray r_i which is represented by a normalised vector $\boldsymbol{v_i}$ which can be decoupled into a part parallel and orthogonal part $\boldsymbol{v_{i,\parallel}}$ and $\boldsymbol{v_{i,\perp}}$ respectively. The ray will refract and follow the path of r_r, which can also be decoupled:

$$\begin{cases} \boldsymbol{v_i} = \boldsymbol{v_{i,\parallel}} + \boldsymbol{v_{i,\perp}} \\ \boldsymbol{v_r} = \boldsymbol{v_{r,\parallel}} + \boldsymbol{v_{r,\perp}} \end{cases}$$

Where $(\boldsymbol{v_{i,\parallel}} \bullet \boldsymbol{v_{i,\perp}}) = (\boldsymbol{v_{r,\parallel}} \bullet \boldsymbol{v_{r,\perp}}) = 0$. Now suppose $\boldsymbol{v_i}$ is known and $\boldsymbol{v_r}$ is to be found. Starting with Snell's law

$$n_1 \sin\theta_i = n_2 \sin\theta_r \tag{A.13}$$

Since the norms of the of tangent parts are equals to the sine - $|\boldsymbol{v_\parallel}| = \frac{|\boldsymbol{v_\parallel}|}{|\boldsymbol{v}|} = \sin\theta$ - , Snell's law can be written as

$$|\boldsymbol{v_{r,\parallel}}| = \frac{n_1}{n_2}|\boldsymbol{v_{i,\parallel}}| \tag{A.14}$$

When combining the fact that $\boldsymbol{v_{i,\parallel}}$ and $\boldsymbol{v_{r,\parallel}}$ are parallel and are in the same orientation, and $\boldsymbol{v_{i,\parallel}} = \boldsymbol{v_i} + \cos\theta_i \boldsymbol{n}$ it is found that

$$\boldsymbol{v_{r,\parallel}} = \frac{n_1}{n_2}(\boldsymbol{v_i} + \cos\theta_i \boldsymbol{n}) \tag{A.15}$$

Using Pythagoras, an expression for the tangent part of the outgoing ray is found

$$\boldsymbol{v_{r,\perp}} = -\sqrt{1 - |\boldsymbol{v_{r,\parallel}}|^2}\boldsymbol{n} \tag{A.16}$$

This gives

$$\boldsymbol{v_r} = \frac{n_1}{n_2}(\boldsymbol{v_i} + \cos\theta_i \boldsymbol{n}) - \sqrt{1 - |\boldsymbol{v_{r,\parallel}}|^2}\boldsymbol{n} \tag{A.17}$$

When recognising $|\boldsymbol{v_{r,\parallel}}| = \sin\theta_r = \frac{n_1}{n_2}\sin\theta_i$, where the second equality uses Snell's law again, the expression for $|\boldsymbol{v_{r,\parallel}}|$ is combined with $\sin\theta^2 + \cos\theta^2 = 1$ to get the expression for the outgoing ray in known parameters:

$$\boldsymbol{v_r} = \frac{n_1}{n_2}\boldsymbol{v_i} + \left(\frac{n_1}{n_2}\cos\theta_i \boldsymbol{n} - \sqrt{1 - \left(\frac{n_1}{n_2}\right)^2 (1 - \cos\theta_i{}^2)}\right)\boldsymbol{n} \tag{A.18}$$

We can simplify $\cos\theta_i$ by

$$\cos\theta_i = \frac{|\boldsymbol{v_{i,\perp}}|}{|\boldsymbol{v_i}|} = |\boldsymbol{v_{i,\perp}}| = (\boldsymbol{v_i} \bullet \boldsymbol{n}) \tag{A.19}$$

And obtain an expression for the outgoing ray in given parameters[5]

$$\boldsymbol{v_r} = \frac{n_1}{n_2}\boldsymbol{v_i} + \left(\frac{n_1}{n_2}(\boldsymbol{v_i} \bullet \boldsymbol{n})\boldsymbol{n} - \sqrt{1 - \left(\frac{n_1}{n_2}\right)^2 (1 - (\boldsymbol{v_i} \bullet \boldsymbol{n})^2)}\right)\boldsymbol{n} \tag{A.20}$$